POLITECNICO DI TORINO

Master Degree course in Mathematical Engineering

Master Degree Thesis

Modelling opinion dynamics on large-scale networks by Boltzmann-type kinetic equations and graphons

Supervisor
Prof. Andrea Tosin

Candidate
Gabriele Taricco

Academic Year 2025-2026

Abstract

This thesis explores the asymptotic behaviour of opinion dynamics on large-scale, heterogeneous networks. To overcome the computational and theoretical challenges posed by the increasing complexity posed by copious amounts of agent interactions, we employ the theory of *graphons* (graph functions) to describe the network topology in the continuous limit. A central contribution of this work is the rigorous derivation of a mean-field kinetic model that generalizes classical spatially homogeneous frameworks to topologically complex settings – by embedding the discrete node set into a continuous domain, we establish the convergence of the discrete particle system to the continuous limit in the Wasserstein-$\mathcal{W}_1$ sense, ensuring that the macroscopic description faithfully retains the structural information of the underlying graph. Moreover, we investigate the analytical characterization of the system's stationary states. Through an analysis of statistical moments, we derive implicit conditions for consensus that reveal the critical dependence of collective behaviour on local network topology – a feature absent in standard mean-field models. Furthermore, we explore the Quasi-Invariant Regime, showing that under specific scaling of the interaction parameters, the non-linear integral collision operator can be approximated by a Fokker-Planck type operator, thereby retrieving standard results in the limit of a connected graph. Finally, the theoretical framework is corroborated through numerical simulations. We quantify the convergence rates of the discrete graphon approximation using the Cut Norm, the Lebesgue L^1 and L^2 norms, and we illustrate the system's time-evolution under simple interaction rules – i.e., the Ochrombel Model – including Bounded Confidence Models. This work provides a robust mathematical foundation for modelling multi-agent systems on graphons, offering new insights into how a networked structure shapes the opinion dynamics.

Contents

Chapter 1

Introduction

1.1 Background

The exchange of ideas, opinions, and beliefs constitutes a fundamental aspect of human society and has historically shaped social structures, cultural development, and collective decision-making. In the contemporary era, these exchanges are increasingly mediated by digital platforms and social networks, which enable large populations of individuals to interact at unprecedented rates and on a global scale. Such platforms facilitate not only the rapid dissemination of information but also the emergence of complex patterns of social influence, opinion formation, and collective behaviour. Understanding these patterns is therefore a central challenge in disciplines ranging from sociology and psychology to the study of network-related dynamics.

In particular, the dynamics of opinion exchange can result in a variety of outcomes. On the one hand, opinions may converge towards a consensus, reflecting social coordination or conformity. On the other hand, interactions may lead to fragmentation into polarized or opposing groups. Alternatively, a high degree of opinion diversity may persist, reflecting the coexistence of multiple viewpoints within a population. Characterizing the conditions under which these outcomes arise, as well as their temporal evolution, is essential for understanding the behaviour of complex social systems.

The implications of such studies extend beyond theoretical inquiry. In political communication, insights into opinion dynamics can inform strategies to address polarization, misinformation, and public engagement. In marketing and innovation, understanding how ideas propagate through social networks can guide targeted interventions strategies. Consequently, research on opinion dynamics and collective behaviour in digitally mediated environments represents a vital interdisciplinary subject, bridging theoretical modelling, empirical analysis and practical applications.

1.2 Opinion Dynamics and Networks

Mathematical models of opinion dynamics aim to capture the mechanisms by which individuals adjust their opinions through interactions with others. Classical models assume that individuals are influenced by compromise with their peers, or by independent sources

such as media exposure.

Since opinions are exchanged within social structures, networks play a fundamental role. Graphs are natural mathematical objects suited to the description of such structures, where vertex $i \in \mathcal{I}$ represents an individual and edge $(i, j) \in \mathcal{E}$ represents an interaction between the agents identified by vertices i and j, respectively. In some cases, interactions are cooperative and lead to alignment of opinions, while in others they are antagonistic, driving individuals further apart [11].

A key difficulty lies in the sheer size of modern social environments: they often involve millions or even billions of individuals. In such cases, graph-theoretical methods quickly become intractable. To address this, recent research has introduced *graphons*, a term that stands for «graph functions». They are continuous limit objects that approximate large graphs in some sense that will be deepened in Section 3.3. Graphons allow one to describe massive networks using measurable functions, which makes the analysis of large-scale opinion dynamics mathematically feasible.

At the same time, kinetic theory offers a statistical framework to study multi-agent systems at scale. By embedding information about the network structure into Boltzmann-type equations, it is possible to analyse how microscopic interactions among agents lead to macroscopic social phenomena.
Recent works have shown that statistical properties of the network, such as the degree distribution, can often provide sufficient information to reproduce collective dynamics (see e.g. [10]). However, the incorporation of graphons enables a more comprehensive and general characterization of the connectivity structure among interacting agents.

1.3 Literature Review and Main Contributions

A significant body of work has explored the modelling of opinion dynamics on networks, particularly within the framework of kinetic models. However, existing approaches often face structural limitations concerning the representation of network connectivity and its probabilistic meaning in the continuous limit. For instance, in the work by [10], a Boltzmann-type model is derived where information about node connectivity is integrated through specific network quantities, without providing an explicit link to the rigorous theory of graphons. While effective, this approach only depicts a partial view, missing the opportunity to leverage the structural power of the graphon theory to consistently track the underlying discrete network. Similarly, other authors, such as those in [4], introduce the use of graphons as an interaction kernel. However, this introduction often relies on an ansatz without a formal justification for the graphon's specific role or its inherent probabilistic meaning as the limit of the discrete network structure.
These gaps in the literature directly motivate the primary objectives of this thesis:

- To rigorously derive a kinetic model for opinion dynamics that fully and explicitly integrates the graphon, indicated by $W(x, x_*)$, as the continuous representation of the network connectivity;
- To leverage this rigorous foundation so as to analyse the convergence of the discrete kinetic equation to the continuous limit equation.

1.4 Structure of the Thesis

The thesis is organized as follows.

Chapter 2 opens with a comprehensive introduction to kinetic theories and Boltzmann-type equations by giving a general but useful background. After that, it is explained how kinetic models can be naturally embedded into social contexts, and the issue about describing the interactions through graphs will be addressed.
Chapter 3 contains a brief yet exhaustive introduction to graph theory. It also includes some motivation as to why the introduction of a limit object is necessary in the context of social dynamics. Finally, it incorporates elements of graphon theory and notions of convergence in ad hoc norms.
Chapter 4 constructs the kinetic model specific to the problem under study and derives the corresponding discrete Boltzmann-type equation. After that, the continuous equation, in the limit $N \to +\infty$, is introduced through a justified ansatz. Lastly, proof of convergence between the solutions of these two equations is given.
Chapter 5 carries out the study of the statistical moments of probability density f. Furthermore, it discusses the existence of equilibrium points to the equation for the average opinion and for the energy of the system. Consequently, it argues about the conditions that have to be met so that consensus among agents is reached. Finally, the Ochrombel simplification of the Sznajd model is implemented in the study of such statistical moments, comparing results with the ones obtained previously.
Chapter 6 contains the derivation of the Quasi Invariant Regime (QIR) for the model that has been constructed, arriving at the determination of the Fokker-Planck (FP) equation. Comparisons with the more standard FP equation of a kinetic model without a graph are conducted.
Chapter 7 is dedicated to numerical simulations. Adopting a simplified interaction scheme based on the Ochrombel model, we visualize the system's evolution and investigate the impact of Bounded Confidence (BC) constraints on consensus formation. The chapter concludes with a numerical validation of the theoretical framework, quantifying the convergence of the discrete graphon approximation W_N to the continuous limit W through a log-log error analysis.
Lastly, Chapter 8 contains a brief summary of the work done and the epilogue of the conclusions reached through this work, plus a description of the still open problems that might be subject of future works.

Chapter 2

Kinetic Models: From Classical Foundations to Networked Systems

As a consequence of the rapid technological developments that have marked the beginning of the twenty-first century, social interactions take place at an unprecedented rate. People across the globe are more connected than ever before, making it so that opinions, ideas and information can travel freely. An effective way of describing the interactions among individuals is to use some sort of networked structures – graphs are likely the most suited mathematical instrument to keep track of such connections. The goal of this thesis is to integrate this graph-based approach with the more standard one based on Kinetic Theories.

2.1 Kinetic Theories Background

In the late 19th century, Ludwig Boltzmann formulated the celebrated integro-differential equation that now bears his name. His primary objective was to derive the macroscopic properties of gases by modelling the underlying microscopic interactions, effectively bridging particle dynamics and statistical mechanics. This approach allowed for the description of systems containing $\mathcal{O}(10^{24})$ particles using a single equation, thereby bypassing the intractable task of solving a massive system of possibly coupled Newton's equations of motion. Following Boltzmann's paradigm, we first consider a spatially homogeneous setting where the microscopic state is described by the stochastic process V_t. We introduce the kinetic probability density function:

$$f = f(v,t) : \mathbb{R} \times [0, +\infty) \to \mathbb{R}. \tag{2.1}$$

The time-evolution of this distribution is governed by the weak form of the Boltzmann equation:

$$\frac{d}{dt} \int_{\mathbb{R}} \varphi(v) f(v,t)\, dv = \int_{\mathbb{R}} \varphi(v) Q(f,f)(v)\, dv, \tag{2.2}$$

which must hold for any suitable test function $\varphi \in \mathfrak{F}$, where $\mathfrak{F}$ is a suitable space of functions that will be discussed later. The term $Q(f, f)$ on the right-hand side represents the *collision operator*, which encodes the mechanism of microscopic interactions between particles. It is worth remarking that the choice of φ represents a crucial degree of freedom in this framework – this flexibility will be exploited thoroughly in the following sections to extract specific physical information from the kinetic model.

2.2 Kinetic Models in Social Dynamics

Throughout the 20-th century researchers have been exploring the realm of kinetic theories. The statistical nature of human behaviours has pushed the research to focus on topics involving social contexts.

Recently, kinetic models have been successfully employed to study the spread of infectious diseases, such as SARS-CoV-2. For instance, the authors in [3] demonstrate how classic compartmental models can be effectively integrated with Boltzmann-type equations. Their approach emphasizes the microscopic description of contact-based interactions among individuals. This granular perspective is crucial for evaluating specific preventive measures and mitigating further disease transmission. Finally, the authors validate the predictive capabilities of their model through numerical simulations, highlighting its practical utility in supporting public health decision-making.

Furthermore, Boltzmann-type equations have been extensively utilized to model the wealth distribution of populations. These kinetic models typically describe the economic state through the exchange of goods and money via binary interactions (see, e.g., [13]). For instance, Bisi [2] investigates a scenario where two distinct populations exhibit specific propensities to trade. The interaction rules are explicitly constructed to incorporate these trading preferences into the transaction dynamics.
A fundamental underlying principle in these models is the conservation of total wealth, which is analogous to the conservation of mass in gas dynamics. A consistent finding across these studies is that wealth is rarely—if ever—uniformly distributed. Instead, the stationary solutions typically exhibit heavy tails, consistent with the well-known Pareto power law.

Finally, kinetic theories have effectively extended into the domain of opinion dynamics, which constitutes the central theme of this thesis (see, e.g., [4, 10]). A distinctive feature of this application is that the topology of interactions is best represented by a graph structure, rather than simple spatial proximity or random mixing. Consequently, the modelling challenge lies not only in defining an appropriate microscopic interaction law but also in coherently embedding this complex network architecture within the classical kinetic framework.

2.3 Social Dynamics on a Networked Structure

Social interactions are intrinsically structured; individuals do not interact randomly with the entire population but rather within a specific web of connections. Consequently, the natural mathematical substrate for modelling such dynamics is a network. In the

discrete setting, this is represented by an undirected graph $\mathcal{G}_N = (\mathcal{I}, \mathcal{E})$, defined by the set of agent indices $\mathcal{I} = \{1, \dots, N\}$ and the set of edges $\mathcal{E}$ representing active connections. To rigorously track the connectivity among agents, we assign an adjacency matrix $A^{(N)} \in \{0,1\}^{N \times N}$ to the graph. The elements of this matrix are defined as:

$$A_{ij}^{(N)} := \begin{cases} 1 & \text{if } (i,j) \in \mathcal{E}, \\ 0 & \text{otherwise.} \end{cases} \tag{2.3}$$

When a connection exists ($A_{ij}^{(N)} = 1$) agents exchange information, updating their internal state. This state is quantified by the *opinion* variable $v \in \mathcal{O} \subset \mathbb{R}$, where $\mathcal{O}$ is a compact set representing the opinion space (e.g., the bounded interval $[-1, 1]$). Consistently with the Boltzmann-Grad limit in classical kinetic theory, we consider only binary interactions. This choice is based upon the standard assumption that, in a sufficiently short time interval, the probability of higher-order interactions – involving three or more agents simultaneously – is negligible.

Accordingly, a generic agent is completely characterized by its composite microscopic state, denoted by the pair (X, V_t). This state vector comprises two distinct components:

1. The Structural State: $X \in \mathcal{I}$ denotes the agent's fixed label or position on the graph $\mathcal{G}_N$. In our framework, the network topology is assumed to be static; therefore, X remains constant over time;

2. The Dynamical State: $V_t : \Omega \to \mathcal{O}$ represents the agent's opinion at time t. Unlike the position, this is a stochastic variable that evolves dynamically through interactions, generating the stochastic process $\{V_t \mid t \in [0, +\infty)\}$.

While this discrete formulation is exact for a fixed population size N, it faces a fundamental barrier. As the number of nodes N grows – approaching the scale of real-world social networks – the adjacency matrix $A^{(N)}$ becomes unwieldy, and the system of N coupled differential equations becomes analytically and computationally intractable. We are thus synonymous with the *many-particle* problem in statistical mechanics: describing the individual trajectory of every particle is neither feasible nor necessary to understand the macroscopic behaviour.

The primary objective of this thesis is to overcome this dimensionality bottleneck. We aim to study the time evolution of the agents' microscopic states by deriving a Boltzmann-type kinetic equation that survives the limit $N \to \infty$. To achieve this, we must replace the discrete, potentially sparse adjacency matrix with a continuous operator that captures the limit properties of the graph structure. This continuous analogue is known as the graphon. The formal introduction of graphons and their integration into the kinetic framework will be the subject of the following chapter.

Chapter 3

Graphons and Continuous Limits

While the discrete graph structure $\mathcal{G}_N$ and its associated adjacency matrix $A^{(N)}$ provide an exact description of finite-sized systems, they become ill-suited for analysis as the population size diverges. To overcome this, we must transition from the discrete algebraic setting to a continuous analytical framework. This convergence is rigorously formalized through the theory of graphons, which provide the limit objects for sequences of dense graphs.

3.1 From the Discrete Setting to the Continuous Limit

To formally bridge the gap between discrete graphs and the continuous graphon concept, we must first embed the set of N vertices into a continuous domain. We consider the vertex set $\mathcal{I} = \{1, 2, \ldots, N\}$. By normalizing these indices with respect to the population size N, we map them to a discrete set of points $\tilde{\mathcal{I}} = \left\{\frac{1}{N}, \frac{2}{N}, \ldots, 1\right\} \subset [0,1]$. We subsequently partition the unit interval $[0, 1]$ into N sub-intervals of equal length $h = \frac{1}{N}$, and we let I_i denote the i-th interval:

$$I_i := \left(\frac{i-1}{N}, \frac{i}{N}\right], \quad \text{for } i = 1, \ldots, N.$$

We define the normalized position $\tilde{x} := \frac{i}{N}$ corresponding to node i. The connectivity of the graph, originally described by the adjacency matrix $A^{(N)}$, can now be lifted to a function on the unit square. We define the piecewise constant graphon W_N as a symmetric, measurable function $W_N : [0,1]^2 \to [0,1]$, such that:

$$W_N(\tilde{x}, \tilde{x}*) := \sum_{i=1}^{N} \sum_{j=1}^{N} A_{ij}^{(N)} \chi_{I_i}(\tilde{x}) \chi_{I_j}(\tilde{x}_*), \tag{3.1}$$

where χ_{I_i} is the characteristic function of the interval I_i, defined as:

$$\chi_{I_i}(\tilde{x}) := \begin{cases} 1 & \text{if } \tilde{x} \in I_i, \\ 0 & \text{otherwise.} \end{cases} \tag{3.2}$$

Note that for the first interval I_1, we include the left boundary 0 to ensure the domain is fully covered (i.e., $I_1 = [0, 1/N]$).

Remark 3.1.1 (Notation Remark)**.** *For the sake of notational cleanliness, from this point forward we will drop the tilde and refer to the continuous variables simply as* $x, x_* \in [0,1]$.

This construction geometrically maps the presence of an edge between vertices (i, j) to a simplified two-dimensional pixel of height and width equal to $\frac{1}{N}$ on the square region $I_i \times I_j$. The resulting function W_N serves as the piecewise constant representation of the discrete graph $\mathcal{G}_N$. The formal definition of a graphon is then recovered by considering the limit of the sequence $\{W_N\}_{N\in\mathbb{N}}$ as $N \to \infty$ in the appropriate norm (typically the Cut Norm or L^2 norm).

Example 3.1.1. *By way of example, we consider the graphon* $W(x, x_*) = \frac{1}{2}(1 - |x - x_*|)$ *[1]. Comparing its two-dimensional representation with a piecewise constant graphon* W_N *that uses* $N = 100$ *nodes we can see what the approximation process looks like:*

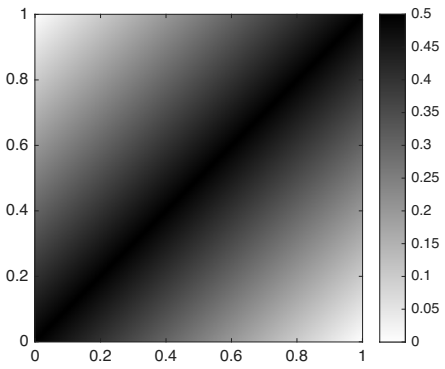

Figure 3.1. Continuous graphon corresponding to $W(x, x_*) = \frac{1}{2}(1 - |x - x_*|)$

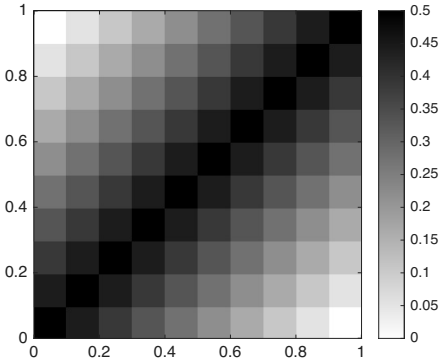

Figure 3.2. Piecewise constant graphon obtained from a discretization of the square $[0,1]^2$ that uses $N = 100$ nodes

3.2 The Graphon: Definition and Associated Operators

Formally, similarly to its piecewise constant representation, a graphon is defined as a symmetric, measurable function:

$$W : [0,1]^2 \to [0,1].$$

Intuitively, this function encodes the limit of the dense graph structure. The value $W(x, x_*)$ represents the probability (or propensity) of a connection existing between two infinitesimal nodes labelled x and x_*. For instance, a constant value $W(x, x_*) = p$ corresponds to the limit of an Erdős-Rényi random graph where every edge exists with independent probability p.

We define the degree function d_W as:

$$\mathrm{d}_W(x) := \int_0^1 W(x, x_*)\, dx_*, \tag{3.3}$$

representing the average connectivity of a node at position x. Another crucial tool for our analysis is the linear operator associated with the kernel W. We define the integral operator $T_W : L^2([0,1]) \to L^2([0,1])$ as:

$$(T_W f)(x) := \int_0^1 W(x, x_*) f(x_*)\, dx_*. \tag{3.4}$$

By the linearity of the integral, this operator satisfies the additive property:

$$T_{W_1+W_2} = T_{W_1} + T_{W_2}.$$

This operator acts as the continuous analogue of the adjacency matrix multiplication. In the context of kinetic theory, the density function f will often depend on additional variables, such as time t or opinion v (i.e., $f = f(x, v, t)$). It is important to note that T_W acts solely on the spatial position variable x_*, treating t and v as parameters.

Finally, the space of graphons is naturally equipped with the operator norm, defined as:

$$\|T_W\|_{2,2} := \sup_{\|f\|_{L^2}=1} \|T_W f\|_{L^2([0,1])},$$

measuring the maximum influence the network structure can exert on a distributed quantity f.

3.3 Convergence of Graphons

Since our objective is to approximate discrete objects (graphs) with continuous limits (graphons), the notion of convergence must be rigorously defined. For dense graphs, the standard metric is the Cut Norm, as it correctly captures structural similarity by "smoothing out" local variations.

Definition 3.3.1 (Cut Norm)**.** *The Cut Norm of a graphon kernel $W \in L^\infty([0,1]^2)$ is defined as:*

$$\|W\|_\square := \sup_{S,T\subseteq[0,1]} \left| \int_{S\times T} W(x, x_*)\, dx dx_* \right|. \tag{3.5}$$

Convergence of a sequence of graphons W_N to W is also understood in this norm: $\|W_N - W\|_\square \to 0$ as $N \to \infty$.

The significance of the Cut Norm is underscored by its relationship with the operator norm. As we will show, convergence in the Cut Norm is equivalent to the convergence of the associated integral operators. This equivalence is fundamental for the kinetic theory

analysis, as it allows us to translate structural approximations of the network into spectral properties of the collision operator. In addition to the Cut Norm, we will employ the standard Lebesgue L^1 and L^2 norms. These latter distances provide stronger metrics that are often easier to compute for the piecewise constant graphons constructed in Section 3.1.

3.3.1 Relationship Between Norms

We now establish the hierarchy of these norms. The following theorem connects the geometric definition of the Cut Norm to the functional analytic definition of the operator norm.

Theorem 3.3.1 (Equivalence of Cut Norm and Operator Norm)**.** *Let W_N and W be graphons. The sequence $\{W_N\}_{N\in\mathbb{N}}$ converges to W in the operator norm if and only if it converges in the Cut Norm. Specifically, there exists a constant $C > 0$ such that:*

$$\|W\|_\square \leq \|T_W\|_{2,2} \leq C\|W\|_\square^{\frac{1}{2}}.$$

Proof. We start by proving the lower bound, $\|W\|_\square \leq \|T_W\|_{2,2}$. For any measurable subsets $S, T \subseteq [0,1]$, we can write the cut integral using indicator functions χ_S and χ_T:

$$\begin{aligned}\left|\int_{S\times T} W(x,y)\,dxdy\right| &= \left|\int_0^1 \chi_S(x)\left(\int_0^1 W(x,y)\chi_T(y),dy\right)dx\right| \\ &= \left|\langle \chi_S, T_W\chi_T\rangle_{L^2([0,1])}\right|.\end{aligned}$$

By the Cauchy-Schwarz inequality and the definition of the operator norm:

$$\begin{aligned}\left|\langle \chi_S, T_W\chi_T\rangle_{L^2([0,1])}\right| &\leq \|\chi_S\|_{L^2}\|T_W\chi_T\|_{L^2([0,1])} \\ &\leq \sqrt{|S|}\cdot\|T_W\|_{2,2}\|\chi_T\|_{L^2([0,1])} \\ &= \sqrt{|S|}\sqrt{|T|}\|T_W\|_{2,2} \leq \|T_W\|_{2,2}.\end{aligned}$$

Since this holds for all subsets $S, T \subseteq [0,1]$, taking the supremum yields:

$$\|W\|_\square \leq \|T_W\|_{2,2}. \tag{3.6}$$

To prove the second inequality, we employ an interpolation argument derived from Janson [6, Lemma E.6].

Step 1: Interpolation via Riesz–Thorin Let $T_W : L^{\mathfrak{p}} \to L^{\mathfrak{q}}$ be the general version of the integral operator associated with the kernel W. We aim to bound its operator norm $\|T_W\|_{\mathfrak{p},\mathfrak{q}}$ by using the Riesz-Thorin Interpolation Theorem.
Let $\theta \in (0,1)$ be an interpolation parameter defined as $\theta := \min(1 - 1/\mathfrak{p}, 1/\mathfrak{q})$. We define the indices $\mathfrak{p}_0, \mathfrak{q}_0$ by the relations:

$$\frac{1}{\mathfrak{p}} = \frac{1-\theta}{\mathfrak{p}_0} \quad \text{and} \quad 1 - \frac{1}{\mathfrak{q}} = (1-\theta)\left(1 - \frac{1}{\mathfrak{q}_0}\right).$$

Provided we consider the complex spaces $L^p([0,1])$, the Riesz–Thorin interpolation theorem yields the bound:

$$\|T_W\|_{\mathfrak{p},\mathfrak{q}} \leq \|T_W\|_{\mathfrak{p}_0,\mathfrak{q}_0}^{1-\theta} \, \|T_W\|_{\mathfrak{p}_1,\mathfrak{q}_1}^{\theta}. \tag{3.7}$$

Step 2: Bounding the Endpoint Norms We now estimate the operator norm at the two endpoints.

- For $(\mathfrak{p}_1, \mathfrak{q}_1) = (\infty, 1)$: The norm $\|T_W\|_{\infty,1}$ corresponds to the «complex cut norm» of the kernel:

  $$\|T_W\|_{\infty,1} = \sup_{\|f\|_\infty, \|g\|_\infty \leq 1} \left| \int W(x,y) f(x) g(y) \, dxdy \right| =: \|W\|_{\square,\mathbb{C}}.$$

  Using Grothendieck's inequality results from Krivine [7], the complex cut norm is comparable to the standard real cut norm $\|W\|_{\square,2}$[1]:

  $$\|W\|_{\square,2} \leq \|T_W\|_{\infty,1} \equiv \|W\|_{\square,\mathbb{C}} \leq \sqrt{2}\|W\|_{\square,2},$$

  with:

  $$\|W\|_{\square,2} := \sup_{\|f\|_\infty, \|g\|_\infty \leq 1} \left| \int_{\Omega^2} W(x,x_*) f(x) g(x_*) \, dxdx_* \right|.$$

  Thus:

  $$\|T_W\|_{\infty,1} \leq \sqrt{2}\|W\|_{\square,2}. \tag{3.8}$$

- For the other endpoint $(\mathfrak{p}_0, \mathfrak{q}_0)$: Assuming the kernel is bounded pointwise by unity ($|W| \leq 1$), the operator maps L^1 to L^∞ with norm at most 1. Since $\|T_W\|_{\mathfrak{p}_0,\mathfrak{q}_0} \leq \|T_W\|_{1,\infty} \leq \|W\|_\infty$, we have:

  $$\|T_W\|_{\mathfrak{p}_0,\mathfrak{q}_0} \leq 1. \tag{3.9}$$

Step 3: Conclusion for the Spectral Norm Substituting (3.8) and (3.9) back into the interpolation inequality (3.7), we obtain:

$$\|T_W\|_{\mathfrak{p},\mathfrak{q}} \leq 1^{1-\theta} \cdot \left(\sqrt{2}\|W\|_{\square,2}\right)^{\theta} = 2^{\theta/2}\|W\|_{\square,2}^{\theta}.$$

[1] This alternative definition of the cut norm, adapted to our work, reads as follows: $\|W\|_{\square,2} := \sup_{\|f\|_\infty, \|g\|_\infty \leq 1} \left| \int_{[0,1]^2} W(x,x_*) f(x) g(x_*) \, dxdx_* \right|$. It is equivalent to the cut norm's definition (3.5) (see [6]).

We specialize this to the case of interest, the spectral operator norm on L^2, by choosing $\mathfrak{p} = \mathfrak{q} = 2$. This yields $\theta = 1/2$. Finally, utilizing the equivalence between the standard cut norm definitions $\|W\|_{\square,2} \leq 4\|W\|_{\square,1}$ (the latter being often denoted simply as $\|W\|_{\square}$), we arrive at the desired bound:

$$\|T_W\|_{2,2} \leq \sqrt{2}\,(4\|W\|_{\square})^{1/2} = 2\sqrt{2}\|W\|_{\square}^{1/2}. \tag{3.10}$$

□

Next, we relate the operator norm – and thus the Cut Norm – to the standard Lebesgue distances.

Proposition 3.3.1 (Hierarchy of Convergence)**.** *For any graphon W, the following chain of inequalities holds:*

$$\|T_W\|_{2,2} \leq \|W\|_{L^2([0,1]^2)} \leq \|W\|_{L^1([0,1]^2)}^{\frac{1}{2}}.$$

Proof. Firstly, we show $\|T_W\|_{2,2} \leq \|W\|_{L^2}$. By definition of the operator norm:

$$\|T_W\|_{2,2}^2 = \sup_{\|f\|_2=1} \|T_W f\|_{L^2}^2 = \sup_{\|f\|_2=1} \int_0^1 \left(\int_0^1 W(x,y) f(y)\, dy \right)^2 dx.$$

Applying the Cauchy-Schwarz inequality to the inner integral:

$$\left(\int_0^1 W(x,y) f(y)\, dy \right)^2 \leq \left(\int_0^1 W(x,y)^2\, dy \right) \left(\int_0^1 (f(y))^2\, dy \right).$$

Since $\|f\|_2 = 1$, substituting this information back into the last integral gives:

$$\|T_W\|_{2,2}^2 \leq \int_0^1 \int_0^1 W(x,y)^2\, dydx = \|W\|_{L^2([0,1]^2)}^2. \tag{3.11}$$

Secondly, we show $\|W\|_{L^2} \leq \|W\|_{L^1}^{\frac{1}{2}}$. Since W is a graphon, it takes values in [0,1]. Consequently, $W(x,y)^2 \leq |W(x,y)|$. Integrating over the square $[0,1]^2$ yields:

$$\|W\|_{L^2([0,1]^2)}^2 = \int_0^1 \int_0^1 W(x,y)^2\, dxdy \leq \int_0^1 \int_0^1 |W(x,y)|\, dxdy = \|W\|_{L^1([0,1]^2)}.$$

Taking the square root concludes the proof. □

Combining Theorem 3.3.1 and Proposition 3.3.1, we observe that:

$$\|W_N - W\|_{\square} \leq \|W_N - W\|_{L^2}.$$

This inequality highlights that Lebesgue L^2 convergence is a stronger condition than cut-norm convergence. While the Cut Norm is the natural metric for graph limits, proving convergence in L^2 (as we will do for the discrete approximation) automatically guarantees convergence of the structural operators.

Chapter 4

Rigorous Derivation of the Continuous Kinetic Model

This chapter constitutes the core of the present work. We begin by establishing the microscopic framework, formally defining the stochastic dynamics of interacting agents on a finite graph. Leveraging classical kinetic theory techniques, we derive the discrete integro-differential equation governing the time evolution of the system.

Subsequently, we introduce the corresponding continuous model, where the discrete network topology is replaced by its limit object, the graphon. This section relies on a specific structural ansatz to bridge the discrete and continuous regimes. This Chapter concludes with a rigorous proof of convergence in the limit $N \to \infty$, demonstrating that the discrete particle system trajectories well-approximate the solutions to the continuous Boltzmann-type equation.

4.1 Preliminary Definitions and Interaction Laws

We begin by establishing the mathematical representation of the system in the discrete setting. Although the population size N is finite, we adopt a functional description that anticipates the continuous limit. We define the empirical probability density $f_N = f_N(x, v, t)$ as:

$$f_N(x, v, t) := \sum_{k=1}^{N} g_k(v, t)\chi_{I_k}(x), \tag{4.1}$$

where $g_k(v, t)$ is the probability density function of the opinion $v \in \mathcal{O}$ for the agent located at node k, and $\chi_{I_k}(x)$ is the spatial indicator function defined in (3.2).

Structurally, f_N is a hybrid function: it is continuous in the opinion variable v but piecewise constant in the network variable x. Physically, it represents a superposition of local probability densities, where the distribution g_k is «smeared» uniformly over the spatial interval I_k corresponding to node k.

Proposition 4.1.1 (Normalization of f)**.** *The function f_N is a valid probability density function.*

Proof. We verify the normalization condition by integrating over the full phase space $[0,1] \times \mathcal{O}$:

$$\int_0^1 \int_{\mathcal{O}} f_N(x,v,t)\, dvdx = \sum_{k=1}^{N} \int_{I_k} \left(\int_{\mathcal{O}} g_k(v,t)\, dv \right) dx = \sum_{k=1}^{N} \frac{1}{N} = 1, \quad \forall t \geq 0,$$

where $\int_{\mathcal{O}} g_k(v,t)\, dv = 1$ owing to the definition of g_k as the probability density distribution of the opinion of the k-th node. Thus, f_N correctly describes the global state of the system. □

Microscopic Interaction Rules

Since the graph topology is assumed to be static, the system dynamics are driven exclusively by changes in the opinion state V_t. We model the binary exchange of information using general interaction laws of the form:

$$\begin{cases} v' & := \Psi(v, v_*, \omega) \\ v'_* & := \Psi^*(v_*, v, \omega). \end{cases} \tag{4.2}$$

Here, v and v_* denote the pre-interaction opinions, while v' and v'_* denote the post-interaction values. The functions $\Psi, \Psi^* : \mathcal{O}^2 \times \Omega \to \mathcal{O}$ define the physics of the exchange (e.g., compromise, alignment, or diffusion). The inclusion of the sample space Ω and the random variable ω allows for stochastic interaction rules, covering a broad class of social dynamics models.

Discrete Time Evolution

The evolution of the system is modelled as a stochastic jump process discretized in time. Over a small time interval Δt, the opinion state of an agent evolves according to:

$$\begin{cases} V_{t+\Delta t} & = (1-\theta)V_t + \theta V'_t \\ V^*_{t+\Delta t} & = (1-\theta)V^*_t + \theta (V^*_t)'. \end{cases} \tag{4.3}$$

The variable θ acts as a stochastic switch determining whether an interaction occurs between agent i (state V) and agent j (state V^*). It is distributed as a Bernoulli random variable:

$$\theta \sim \text{Bernoulli}\left(W_N(X_i, X_j)\Delta t\right).$$

This definition encapsulates two key features of the dynamics:

1. Topology: If agents i and j are not connected, then $W_N(X_i, X_j) = 0$, implying $\theta = 0$ with certainty. No interaction can occur;
2. Rate Scaling: The probability of interaction scales linearly with Δt. This ensures that in the continuous limit $\Delta t \to 0$, the process recovers a standard kinetic rate equation.

Validity of the Interaction Laws

For the kinetic model to be physically consistent, it is imperative that the interaction laws preserve the domain of definition. That is, given pre-interaction opinions $v, v_* \in \mathcal{O}$, the post-interaction state v' must remain within $\mathcal{O}$ almost surely.

Consider a general linear interaction rule of the form:

$$v' = pv + qv_*,$$

where p and q are scalar coefficients that may depend on stochastic variables. Without loss of generality, let us consider a symmetric bounded domain $\mathcal{O} = [-a, a]$ with $a > 0$. To ensure $v' \in \mathcal{O}$, we require $|v'| \leq a$.
Using the triangle inequality, we observe:

$$|v'| = |pv + qv_*| \leq |p||v| + |q||v_*| \leq a(|p| + |q|).$$

Consequently, a sufficient condition to guarantee $|v'| \leq a$ is:

$$|p| + |q| \leq 1. \tag{4.4}$$

It is important to note that if p and q are stochastic, this inequality must hold for every realization of the random variables, not merely for their expectations. If the coefficients are non-negative ($p, q \geq 0$), Condition (4.4) simplifies to $p+q \leq 1$, meaning the interaction is a convex combination (possibly with dissipation).

Example 4.1.1 (Stochastic Interaction Weights)**.** *To illustrate this, let $\mathcal{O} = [-1, 1]$ and consider the following specific structure for the interaction coefficients:*

$$p = 1 - \eta C_1, \quad q = \eta C_2,$$

where $C_1, C_2 \in \mathbb{R}$ are deterministic parameters and $\eta \in [0, 1]$ is a stochastic variable. The post-interaction state is thus:

$$v' = (1 - \eta C_1)v + \eta C_2 v_*.$$

We seek the conditions on C_1 and C_2 that ensure $v' \in \mathcal{O}$ for all possible realizations of η. First, we assume the coefficients are non-negative to interpret the process as a weighted compromise.

- *For $q \geq 0$, we require $C_2 \geq 0$ (since $\eta \geq 0$);*
- *For $p \geq 0$, we require $1 - \eta C_1 \geq 0$. Since η can reach 1, we must have $C_1 \leq 1$.*

Next, we impose the stability condition $p + q \leq 1$:

$$\begin{aligned} &(1 - \eta C_1) + \eta C_2 \leq 1 \\ \implies\ &1 + \eta(C_2 - C_1) \leq 1 \\ \implies\ &\eta(C_2 - C_1) \leq 0. \end{aligned}$$

Since η is non-negative and can be non-zero, this implies $C_2 - C_1 \leq 0$, or $C_2 \leq C_1$. Combining these requirements, the necessary parameter range for domain preservation is:

$$0 \leq C_2 \leq C_1 \leq 1.$$

4.2 Notions of Convergence: the Wasserstein Metric

To rigorously quantify the convergence of the discrete empirical measure to its continuous limit, we require a metric that respects the geometry of the underlying state space. The standard choice in kinetic theory and mean-field limits is the Wasserstein distance, often referred to as the "Earth Mover's Distance."

Definition 4.2.1 (Wasserstein Metric)**.** *Let $(\mathcal{Z}, d)$ be a complete separable metric space, and let $\mathcal{P}_p(\mathcal{Z})$ denote the space of probability measures on $\mathcal{Z}$ with finite p-th moment. The p-th Wasserstein distance between two measures $\mu, \nu \in \mathcal{P}_p(\mathcal{Z})$ is defined as:*

$$\mathcal{W}_p(\mu, \nu) := \left(\inf_{\gamma \in \Gamma(\mu,\nu)} \int_{\mathcal{Z}\times\mathcal{Z}} d(z, z_*)^p \, d\gamma(z, z_*) \right)^{\frac{1}{p}}, \tag{4.5}$$

where $\Gamma(\mu, \nu)$ is the set of all couplings of μ and ν — i.e., joint probability measures γ on $\mathcal{Z} \times \mathcal{Z}$ whose marginals are μ and ν, respectively.

In this work, we will primarily utilize the 1-Wasserstein distance ($p = 1$), which simplifies to:

$$\mathcal{W}_1(\mu, \nu) := \inf_{\gamma \in \Gamma(\mu,\nu)} \int_{\mathcal{Z}\times\mathcal{Z}} d(z, z_*) \, d\gamma(z, z_*). \tag{4.6}$$

Physical Interpretation: The Earth Mover's Analogy The Wasserstein distance admits an intuitive physical interpretation. Consider μ and ν as two piles of dirt (distributions of mass) with different shapes but equal total volume. The quantity $\mathcal{W}_1(\mu, \nu)$ represents the minimum mechanical work required to transport the mass from the configuration μ to the configuration ν. The "cost" of moving a unit of mass is proportional to the distance travelled. It is heuristically defined as:

$$\text{Wasserstein Metric} = \text{minimum}(\text{Mass Moved} \times \text{Average Distance Moved}).$$

Comparison with Other Metrics Alternative metrics, such as the Total Variation (TV) distance or the Kullback-Leibler (KL) divergence, are often insufficient for problems involving particle transport. Total Variation measures the pointwise discrepancy between densities. If two distributions have disjoint supports (e.g., two Dirac deltas δ_0 and δ_ϵ), the TV distance is constant ($= 2$) regardless of how close they are spatially. Wasserstein Distance, in contrast, incorporates the metric structure of the space. For the same Dirac

deltas, $\mathcal{W}_1(\delta_0, \delta_\epsilon) = \epsilon$. Thus, the Wasserstein metric allows us to quantify the convergence rate of a discrete measure to a continuous one even when they have completely different supports.

Finally, we state a fundamental duality result that facilitates the estimation of the Wasserstein distance without explicitly constructing the actual coupling.

Theorem 4.2.1 (Kantorovich-Rubinstein Duality)**.** *Let μ, ν be probability measures on a metric space $\mathcal{Z}$. Then:*

$$\mathcal{W}_1(\mu, \nu) = \sup_{\varphi \in \mathrm{Lip}_1(\mathcal{Z})} \int_{\mathcal{Z}} \varphi(z) d(\mu - \nu)(z), \tag{4.7}$$

where the supremum is taken over all 1*-Lipschitz continuous, scalar functions $\varphi : \mathcal{Z} \to \mathbb{R}$.*

This dual formulation transforms the minimization problem over couplings into a maximization problem over test functions, which is typically more tractable for kinetic equations.

4.3 Derivation of the Discrete Equation and Statement of the Continuous Limit

Prior to deriving the kinetic equation, we establish the following notational conventions to streamline the analysis. Let $\mathcal{A}$ denote the global phase space of the system, defined as the Cartesian product of the normalized network domain and the opinion space:

$$\mathcal{A} := [0,1] \times \mathcal{O}.$$

Furthermore, in the context of binary interactions, it is necessary to distinguish between the state of the test agent and that of the field agent. Accordingly, we adopt the following shorthand notation:

$$f_N(t) \equiv f_N(x, v, t), \qquad f_N^*(t) \equiv f_N(x_*, v_*, t).$$

Here, the asterisk indicates that the distribution is evaluated at the coordinates (x_*, v_*, t) of the interacting partner. However, for the sake of clarity the extended version of this notation will be adopted whenever necessary.

Let Φ be a suitable smooth test function. We analyse the time evolution of the observable $\Phi(X, V_t)$. The stochastic update rule (4.3) involves two distinct sources of randomness: the selection of interacting pairs (governed by the Bernoulli variable θ) and the outcome of the interaction itself (governed by the sample variable ω).

We first compute the expectation with respect to the Bernoulli trial, conditioned on the current state (X, V_t) and a specific partner (X^*, V_t^*). Recalling that $\theta \sim \text{Bernoulli}(W_N(X, X^*)\Delta t)$, we have:

$$\mathbb{E}\Big[\Phi(X, V_{t+\Delta t})\Big] = \mathbb{E}\Big[\Phi(X, V_t)(1 - W_N(X, X^*)\Delta t) + \Phi(X, V_t')W_N(X, X^*)\Delta t\Big]$$

Note that in the second term, $V' = \Psi(V_t, V_t^*, \omega)$ remains a random variable depending on the interaction noise ω.
Rearranging the terms to form the difference quotient:

$$\frac{\mathbb{E}\Big[\Phi(X, V_{t+\Delta t})\Big] - \mathbb{E}\Big[\Phi(X, V_t)\Big]}{\Delta t} = \mathbb{E}\Big[W_N(X, X^*)\left(\Phi(X, V_t') - \Phi(X, V_t)\right)\Big]$$

Taking the limit $\Delta t \to 0$ and applying the same logic to the field agent (X^*, V_t^*), we obtain the following system of equations:

$$\begin{cases} \dfrac{d}{dt}\mathbb{E}\Big[\Phi(X, V_t)\Big] & = \mathbb{E}\Big[W_N(X, X^*)\left(\Phi(X, V_t') - \Phi(X, V_t)\right)\Big] \\ \dfrac{d}{dt}\mathbb{E}\Big[\Phi(X^*, V_t^*)\Big] & = \mathbb{E}\Big[W_N(X, X^*)\left(\Phi(X^*, (V_t')^*) - \Phi(X^*, V_t^*)\right)\Big]. \end{cases} \tag{4.8}$$

Following the same reasoning as in [10], we observe that the pairs (X, V_t) and (X^*, V_t^*) represent generic agents within the same population. Consequently, they are governed by identical probability laws. This indistinguishability implies that the expectation of any observable is invariant under particle exchange, specifically $\mathbb{E}[\Phi(X, V_t)] = \mathbb{E}[\Phi(X^*, V_t^*)]$. Leveraging this symmetry, we combine the coupled equations to obtain:

$$\frac{d}{dt}\mathbb{E}\Big[\Phi(X^*, V_t^*)\Big] = \frac{1}{2}\mathbb{E}\Big[W_N(X, X^*)\left(\Phi(X, V_t') + \Phi(X^*, (V_t')^*) - \Phi(X, V_t) - \Phi(X^*, V_t^*)\right)\Big].$$

After expanding the expectation operator with respect to the empirical distribution f_N, we recover the Discrete Boltzmann Equation:

$$\begin{aligned} \frac{d}{dt}\int_0^1 \int_{\mathcal{O}} \Phi(x, v) f_N(t) dv dx = \iint_{[0,1]^2} \iint_{\mathcal{O}^2} & W_N(x, x_*) \\ & \times \frac{1}{2}\langle \Phi(x, v') + \Phi(x_*, v_*') - \Phi(x, v) - \Phi(x_*, v_*)\rangle f_N(t) f_N^*(t)\, dv dv_*\, dx dx_* \end{aligned} \tag{4.9}$$

Here, the angle brackets $\langle\cdot\rangle$ formally represent the integral over the probability space Ω of the interaction parameters.

Statement of the Continuous Limit

We now propose the continuous counterpart to (4.9), which acts as the mean-field limit as $N \to \infty$. By formally replacing the discrete empirical density f_N with the continuous density f, and the step-function graphon W_N with the limit graphon W, we obtain the ansatz for the Continuous Boltzmann-Type Equation:

$$\begin{aligned} \frac{d}{dt}\int_0^1 \int_{\mathcal{O}} \Phi(x, v) f(t) dv dx = \iint_{[0,1]^2} \iint_{\mathcal{O}^2} & W(x, x_*) \\ & \times \frac{1}{2}\langle \Phi(x, v') + \Phi(x_*, v_*') - \Phi(x, v) - \Phi(x_*, v_*)\rangle f(t) f^*(t)\, dv dv_*\, dx dx_* \end{aligned} \tag{4.10}$$

The rigorous justification of this ansatz – specifically, proving that the solution to (4.9) converges to the solution of (4.10) in the Wasserstein metric – is the primary focus of the remainder of this chapter.

4.4 Proof of Convergence

The rigorous validation of the mean-field limit requires demonstrating that the empirical distribution f_N, governed by the discrete dynamics (4.9), converges to the solution f of the continuous Equation (4.10) as the population size diverges.

In this section, we present two complementary convergence results, distinguishing between the analytic tools employed:

1. Lebesgue L^2-norm Convergence: We first establish convergence assuming the interaction kernel W_N converges in the standard Lebesgue L^2-norm. This approach offers a direct proof but relies on stronger regularity assumptions on the graph sequence;

2. Cut Norm plus Lebesgue L^1-norm Convergence: We then provide a more general result that integrates the Cut Norm. By leveraging the norm equivalence established in Chapter 3 (Theorem 3.3.1), we show that convergence holds even when the graph sequence converges only in the structural sense, a critical feature for sparse or random graph limits. Without further assumptions, the Cut Norm alone is not enough to guarantee appropriate convergence and the Lebesgue L^1-norm must be brought into the formulation;

3. Cut Norm Convergence: We provide as last result the purest formulation we obtained – with an additional hypothesis on the rate of convergence of W_N to W we showed that the Cut Norm alone can be sufficient to ensure rigorous convergence.

4.4.1 Convergence in the L^2 Norm (First Result)

We begin by invoking the standard assumption of particle exchangeability. In kinetic theory, the indistinguishability of interacting agents allows us to exploit the symmetry of the binary interaction. Specifically, the contribution of the field agent (x_*, v_*) to the total energy change is statistically equivalent to that of the test agent (x, v) when integrated over the phase space.

Consequently, the interaction kernel in the weak formulations (4.9) and (4.10) simplifies as follows:

$$\frac{1}{2}\langle \Phi(x, v') + \Phi(x_*, v'_*) - \Phi(x, v) - \Phi(x_*, v_*)\rangle = \langle \Phi(x, v') - \Phi(x, v)\rangle.$$

This reduction significantly streamlines the analysis. Accordingly, the discrete and continuous governing equations can be restated in the following compact forms:

$$\frac{d}{dt}\int_0^1 \int_{\mathcal{O}} \Phi(x, v) f_N(t) dv dx = \iint_{[0,1]^2} \iint_{\mathcal{O}^2} W_N(x, x_*)\langle \Phi(x, v') - \Phi(x, v)\rangle f_N(t) f_N^*(t)\, dv dv_*\, dx dx_*, \tag{4.11}$$

(4.12)
$$\frac{d}{dt}\int_0^1\int_{\mathcal{O}}\Phi(x,v)f(t)dvdx=\iint_{[0,1]^2}\iint_{\mathcal{O}^2}W(x,x_*)\langle\Phi(x,v')-\Phi(x,v)\rangle f(t)f^*(t)\,dvdv_*\,dxdx_*.$$

Subtracting Equation (4.12) to Equation (4.11) we obtain:

$$\frac{d}{dt}\int_0^1\int_{\mathcal{O}}\Phi(x,v)\left(f_N(t)-f(t)\right)dvdx=\int_0^1\int_0^1\int_{\mathcal{O}}\int_{\mathcal{O}}\left(\Phi(x,v')-\Phi(x,v)\right)\\ \times\left(W_N(x,x_*)f_N(t)f_N^*(t)-W(x,x_*)f(t)f^*(t)\right)\,dvdv_*\,dxdx_*.$$

Integrating both sides in time over the generic interval $[0,t]$ we get:

$$\int_0^1\int_{\mathcal{O}}\Phi(x,v)\left(f_N(t)-f(t)\right)\,dvdx=\int_0^1\int_{\mathcal{O}}\Phi(x,v)\left(f_N(0)-f(0)\right)\,dvdx\\ +\int_0^t\left[\int_0^1\int_0^1\int_{\mathcal{O}}\int_{\mathcal{O}}\left(\Phi(x,v')-\Phi(x,v)\right)\left(W_Nf_N(s)f_N^*(s)-Wf(s)f^*(s)\right)\,dvdv_*\,dxdx_*\right]ds.$$

Focusing on the right-hand side, and specifically on the second factor of the last integral, we observe that it admits the following representation:

$$\begin{aligned}W_Nf_Nf_N^*-Wff^*&=W_Nf_Nf_N^*-Wff^*+Wf_Nf_N^*-Wf_Nf_N^*+Wf_Nf^*-Wf_Nf^*\\&=f_Nf_N^*(W_N-W)+Wf_N(f_N^*-f^*)+Wf^*(f_N-f).\end{aligned}$$

Taking the modulus and substituting the resulting expression into the formulation yields:

(4.13)
$$\begin{aligned}\left|\int_0^1\int_{\mathcal{O}}\Phi(x,v)\left(f_N(t)-f(t)\right)dvdx\right|&\le\underbrace{\left|\int_0^1\int_{\mathcal{O}}\Phi(x,v)\left(f_N(0)-f(0)\right)dvdx\right|}_{①}\\&+\int_0^t\underbrace{\left|\int_0^1\int_0^1\int_{\mathcal{O}}\int_{\mathcal{O}}(\Phi(x,v')-\Phi(x,v))f_N(s)f_N^*(s)\left(W_N-W\right)dvdv_*dxdx_*\right|}_{②}ds\\&+\int_0^t\underbrace{\left|\int_0^1\int_0^1\int_{\mathcal{O}}\int_{\mathcal{O}}(\Phi(x,v')-\Phi(x,v))Wf_N(s)\left(f_N^*(s)-f^*(s)\right)dvdv_*dxdx_*\right|}_{③}ds\\&+\int_0^t\underbrace{\left|\int_0^1\int_0^1\int_{\mathcal{O}}\int_{\mathcal{O}}(\Phi(x,v')-\Phi(x,v))Wf^*(s)\left(f_N(s)-f(s)\right)dvdv_*dxdx_*\right|}_{④}ds.\end{aligned}$$

To address the definition of the space of test functions from which we draw $\Phi(x,v)$, notice that the left-hand side and the first term of the right-hand side are characterized

by a structure similar to the formulation from Theorem 4.2.1. Therefore, we can choose $\Phi \in \mathrm{Lip}_1(\mathcal{A})$.

In order to perform the actual estimates, let us give the following useful remark.

Remark 4.4.1 (Boundedness of function Φ)**.** *It is valuable to observe that a such chosen function $\Phi \in \mathrm{Lip}_1(\mathcal{A})$ is bounded. Indeed:*

$$|\Phi(x_1, v_1) - \Phi(x_2, v_2)| \leq \mathrm{d}\left((x_1, v_1), (x_2, v_2)\right) \leq \mathrm{Diam}(\mathcal{A})$$

Assuming that $\mathcal{O}$ is a compact set of the form $[-a, a]$, for some $a > 0$, and using the Euclidean distance, we obtain: $\mathrm{Diam}(\mathcal{A}) = \sqrt{1 + 4a^2}$*. Now:*

$$\begin{aligned}\|\Phi\|_{L^\infty} &= \sup_{(x,v)\in\mathcal{A}} |\Phi(x, v)| = \sup_{(x,v)\in\mathcal{A}} |\Phi(x, v) - \Phi(x_1, v_1) + \Phi(x_1, v_1)| \\ &\leq \sup_{(x,v)\in\mathcal{A}} (|\Phi(x, v) - \Phi(x_1, v_1)|) + |\Phi(x_1, v_1)|\end{aligned}$$

Owing to function Φ being Lipschitz and the resulting arbitrariness in choosing point (x_1, v_1), we can take it in such a way that $|\Phi(x_1, v_1)| \leq b$, $b > 0$. By doing so we get:

$$\|\Phi\|_{L^\infty(\mathcal{A})} \leq \sqrt{1 + 4a^2} + b =: \mathrm{C} \tag{4.14}$$

Now, let us consider the right-hand side of inequality (4.13).

Term ① The Term ① of the inequality (4.13) is to be left unchanged – this term will give rise to the Wasserstein $\mathcal{W}_1$ metric between the initial data of functions f_N and f.

Term ② Exploiting the bound in (4.14), term ② can be estimated as follows:

$$\begin{aligned}② &\leq 2\|\Phi\|_{L^\infty(\mathcal{A})} \int_0^1 \int_0^1 |W_N - W| \int_{\mathcal{O}} f_N(s)dv \int_{\mathcal{O}} f_N^*(s)dv_* \, dxdx_* \\ &\leq 2\mathrm{C}\left(\int_0^1 \int_0^1 |W_N - W|^2 dxdx_*\right)^{\frac{1}{2}} \left(\int_0^1 \int_0^1 F_N^2(x, s)F_N^2(x_*, s)dxdx_*\right)^{\frac{1}{2}} \\ &= 2\mathrm{C}\|F_N(s)\|^2_{L^2([0,1])}\|W_N - W\|_{L^2([0,1]^2)},\end{aligned}$$

where we have introduced the marginal distribution of f_N with respect to the spatial variable $x \in [0,1]$ as $F_N(x, t) := \int_{\mathcal{O}} f_N(x, v, t)dv$.

Remark 4.4.2. *Notice that, by choosing $\Phi(x, v) = \varphi(x)$ and substituting back into Equation (4.9), we obtain:*

$$\frac{d}{dt}\int_0^1 \varphi(x)\int_{\mathcal{O}} f_N(x,v,t)dvdx = 0, \quad \forall \varphi(x) \in \mathrm{Lip}_1([0,1]).$$

It is easy to see that this implies:

$$\frac{\partial F_N}{\partial t}(x,t) = 0,$$

whence: $F_N(x,t) \equiv F_N(x,0)$. *An explicit computation leads us to conclude that:*

$$\begin{aligned} F_N(x,t) = F_N(x,0) = \int_{\mathcal{O}} f_N(x,v,0)dv &= \int_{\mathcal{O}} \sum_{k=1}^{N} g_k(v,0)\chi_{I_k}(x)dv \\ &= \sum_{k=1}^{N} \chi_{I_k}(x)\left(\underbrace{\int_{\mathcal{O}} g_k(v,0)dv}_{=1,\ \mathrm{HP}}\right) = 1, \forall x \in [0,1], \end{aligned}$$

finally implying that $\|F_N(x,t)\|^2_{L^2([0,1])} = 1$.

This observation allows us to conclude that:

$$\textcircled{2} \leq 2\mathrm{C}\|W_N - W\|_{L^2([0,1]^2)}.$$

Term ③ The goal is to bring the term labelled as ③ into a form similar to that of the formulation of Theorem 4.2.1. We have:

$$\textcircled{3} = \left| \int_0^1 \int_{\mathcal{O}} \underbrace{\left[\int_0^1 \int_{\mathcal{O}} (\Phi(x,v') - \Phi(x,v)) W(x,x_*) f_N(s)\, dvdx \right]}_{:= a(x_*,v_*)} (f_N^*(s) - f^*(s))\, dv_* dx_* \right|.$$

Starting from function $a(x_*, v_*)$, we want to define another function $\tilde{a}(x_*, v_*)$, scaling function a by its Lipschitz constant, such that $\tilde{a} \in \mathrm{Lip}_1(\mathcal{A})$. First, we need to prove that function a itself is Lipschitz continuous. First, let us observe that $a(x_*, v_*)$ is a continuous function in both its arguments due to a corollary of the Fundamental theorem of Calculus. Moreover, some assumptions need to be made both on the kernel W and on the interaction map Ψ. Such hypotheses are:

- $\Phi \in \mathrm{Lip}_1(\mathcal{A})$, already stated previously;
- $W(x,\cdot) \in \mathrm{Lip}_{L_W}([0,1])$, uniformly in x, with $L_W > 0$;
- $\Psi(v,\cdot,\omega) \in \mathrm{Lip}_{L_\Psi}(\mathcal{O})$, uniformly in v and ω, with $L_W > 0$.

Under these assumptions we have:

$$\begin{aligned}
a(x_1,v_1)-a(x_2,v_2) &= \int_0^1\int_{\mathcal{O}} \big[\Phi(x,\Psi(v,v_1,\omega))-\Phi(x,v)\big]W(x,x_1)f_N(s)dxdv \\
&\quad -\int_0^1\int_{\mathcal{O}} \big[\Phi(x,\Psi(v,v_2,\omega))-\Phi(x,v)\big]W(x,x_2)f_N(s)dvdx \\
&= \int_0^1\int_{\mathcal{O}} \Big[\Phi(x,\Psi(v,v_1,\omega))W(x,x_1)-\Phi(x,v)W(x,x_1) \\
&\qquad -\Phi(x,\Psi(v,v_2,\omega))W(x,x_2)+\Phi(x,v)W(x,x_2) \\
&\qquad -\Phi(x,\Psi(v,v_2,\omega))W(x,x_1)+\Phi(x,\Psi(v,v_2,\omega))W(x,x_1)\Big]f_N(s)dvdx \\
&= \int_0^1\int_{\mathcal{O}} \Big[\Phi(x,\Psi(v,v_1,\omega))-\Phi(x,\Psi(v,v_2,\omega))\Big]W(x,x_1)f_N(s)dvdx \\
&\quad +\int_0^1\int_{\mathcal{O}} \Big[W(x,x_1)-W(x,x_2)\Big]\Phi(x,\Psi(v,v_2,\omega))f_N(s)dvdx \\
&\quad +\int_0^1\int_{\mathcal{O}} \Big[W(x,x_2)-W(x,x_1)\Big]\Phi(x,v)f_N(s)dvdx.
\end{aligned}$$

Taking the absolute values of both sides:

$$\begin{aligned}
\Big|a(x_1,v_1)-a(x_2,v_2)\Big| &\le \int_0^1\int_{\mathcal{O}} \Big|\Phi(x,\Psi(v,v_1,\omega))-\Phi(x,\Psi(v,v_2,\omega))\Big|W(x,x_1)f_N(s)\,dvdx \\
&\quad +\int_0^1\int_{\mathcal{O}} \Big|W(x,x_1)-W(x,x_2)\Big|\Big|\Phi(x,\Psi(v,v_2,\omega))\Big|f_N(s)\,dvdx \\
&\quad +\int_0^1\int_{\mathcal{O}} \Big|W(x,x_2)-W(x,x_1)\Big|\Big|\Phi(x,v)\Big|f_N(s)\,dvdx.
\end{aligned}$$

Leveraging our hypotheses, alongside the uniform boundedness of the graphon ($W(x,x_*)\le 1$) and the conservation of mass ($\int_0^1\int_{\mathcal{O}} f_N(s)\,dxdv=1$), we obtain:

$$\begin{aligned}
\Big|a(x_1,v_1)-a(x_2,v_2)\Big| &\le \int_0^1\int_{\mathcal{O}} \Big|\Psi(v,v_1,\omega)-\Psi(v,v_2,\omega)\Big|f_N(s)\,dvdx+\mathrm{CL}_W|x_1-x_2|+\mathrm{CL}_W|x_1-x_2| \\
&\le 2\mathrm{CL}_W|x_1-x_2|+L_\Psi|v_1-v_2|,
\end{aligned}$$

hence:

$$\mathrm{Lip}(a)\le \max(2\mathrm{CL}_W, L_\Psi).$$

We can then define:

$$\tilde{a}(x_*,v_*) := \frac{a(x_*,v_*)}{\max(2\mathrm{CL}_W, L_\Psi)} \in \mathrm{Lip}_1(\mathcal{A}). \tag{4.15}$$

Finally, Term ③ becomes:

$$
\begin{aligned}
③ &\leq \left| \int_0^1 \int_{\mathcal{O}} \max(2\mathrm{CL}_W, L_\Psi) \tilde{a}(x_*, v_*) \Big[f_N^*(s) - f^*(s) \Big] dv_* dx_* \right| \\
&\leq \max(2\mathrm{CL}_W, L_\Psi) \sup_{\tilde{a} \in \mathrm{Lip}_1(\mathcal{A})} \left| \int_0^1 \int_{\mathcal{O}} \tilde{a}(x_*, v_*) \Big[f_N^*(s) - f^*(s) \Big] dv_* dx_* \right| \\
&= \tilde{k} \mathcal{W}_1(f_N(s), f(s)),
\end{aligned} \tag{4.16}
$$

where $\tilde{k} := \max(2\mathrm{CL}_W, L_\Psi)$.

Term ④ This last term has a similar structure to Term ③, aside from the fact that function a takes the form:

$$
a(x_*, v_*) = \left[\int_0^1 \int_{\mathcal{O}} (\Phi(x, v') - \Phi(x, v)) W(x, x_*) f(s) dv dx \right].
$$

Without further hypotheses, we can define function $\tilde{a}$ in the same way since $\mathrm{Lip}(a)$ for term ④ is the same as the one for term ③. Therefore, we finally get:

$$
④ \leq \tilde{k} \mathcal{W}_1(f_N(s), f(s)). \tag{4.17}
$$

Substituting these estimates back into inequality (4.13) and taking the $\sup_{\Phi \in \mathrm{Lip}_1(\mathcal{A})}$ operator we obtain:

$$
\begin{aligned}
\mathcal{W}_1(f_N(t), f(t)) \leq \mathcal{W}_1(f_N(0), f(0)) &+ 2\mathrm{C}t \|W_N - W\|_{L^2([0,1]^2)} \\
&+ \int_0^t 2\tilde{k} \mathcal{W}_1(f_N(s), f(s)) ds.
\end{aligned} \tag{4.18}
$$

With the idea of applying Grönwall's inequality, we can define the following quantities:

$$
\begin{aligned}
\alpha(t) &:= \mathcal{W}_1(f_N(0), f(0)) + 2\mathrm{C}t \|W_N - W\|_{L^2([0,1]^2)} \\
\beta(s) &:= 2\tilde{k} \\
u(t) &:= \mathcal{W}_1(f_N(t), f(t)).
\end{aligned}
$$

Observing that the time derivative is non-negative:

$$
\frac{d}{dt} \alpha(t) = 2C \|W_N - W\|_{L^2([0,1]^2)} \geq 0,
$$

we conclude that $\alpha(t)$ is a non-decreasing function. This monotonicity allows us to apply the simplified form of Grönwall's inequality. Thus:

$$\begin{cases} \mathcal{W}_1(f_N(t), f(t)) \leq e^{2\tilde{k}t}\Big[\mathcal{W}_1(f_N(0), f(0)) + \mathrm{A}(t)\|W_N - W\|_{L^2([0,1]^2)}\Big] \\ \text{where:} \quad A(t) = 2\mathrm{C}t, \quad \tilde{k} := \max(2\mathrm{CL}_W, L_\Psi). \end{cases} \tag{4.19}$$

Since the derived pointwise estimate holds for any arbitrary finite time horizon $T > 0$, we can establish a uniform bound over the compact interval $[0, T]$. Consequently, taking the supremum of the Wasserstein distance over $t \in [0, T]$ yields the following finite-time stability estimate:

$$\begin{cases} \sup\limits_{t\in[0,T]} \mathcal{W}_1(f_N(t), f(t)) \leq e^{2\tilde{k}T}\Big[\mathcal{W}_1(f_N(0), f(0)) + A(T)\|W_N - W\|_{L^2([0,1]^2)}\Big], \\ \text{where:} \quad A(T) = 2\mathrm{C}T, \quad \tilde{k} := \max(2\mathrm{CL}_W, L_\Psi). \end{cases} \tag{4.20}$$

Remark 4.4.3. *It is mathematically sound to first apply the supremum over $\tilde{a}$ to bound terms ③ and ④, and subsequently apply the supremum over Φ to derive the final estimate. Indeed, let $G(\Phi)$ denote the functional of interest and $K(\Phi, \tilde{a})$ the upper bound derived from the interaction terms. We observe that:*

$$G(\Phi) \leq K(\Phi, \tilde{a}) \leq \sup_{\tilde{a},\Phi} K(\Phi, \tilde{a}) =: \bar{K}, \quad \forall \Phi,$$

from which it immediately follows that:

$$G(\Phi) \leq \bar{K} \implies \sup_{\Phi} G(\Phi) \leq \bar{K}.$$

The arbitrary nature of the test function Φ represents a crucial degree of freedom in this argument, ensuring that the uniform bound holds effectively across the entire function space.

4.4.2 Convergence in the combination of L^1 Norm and Cut Norm (Second Result)

This second convergence result differs from the analysis presented in Section 4.4.1 primarily in the treatment of the Term ②. This alternative derivation is motivated by the recognized relevance of the Cut Norm ($\|\cdot\|_\square$) in the theory of graphons, as opposed to the Lebesgue L^2-norm, which is often considered a non-standard choice for analysing convergence in this class of graph limit problems (see, for instance, [11]). Nevertheless, due to the complexity of the non-linear terms involved in the kinetic equations and the fact that the Cut Norm is generally weaker than the Lebesgue norms (i.e., convergence in the Cut Norm does not imply convergence in Lebesgue L^1- or L^2-norms), a purely Cut Norm approach is insufficient. Therefore, we utilize a combination of the Cut Norm and the Lebesgue L^1-norm to establish the convergence proof rigorously. This methodology allows us to fully leverage the structural convergence granted by the Cut Norm while ensuring the necessary analytical strength provided by the Lebesgue L^1 space.

Term ② can be reformulated as:

$$② = \left| \int_0^1 \int_0^1 (W_N(x, x_*) - W(x, x_*)) \underbrace{\int_{\mathcal{O}} \int_{\mathcal{O}} (\Phi(x, v') - \Phi(x, v)) f_N(s) f_N^*(s) dv dv_*}_{:=\xi(x, x_*, s)} dx dx_* \right|$$

Recalling the definition of the integral operator in (3.4), we can easily see that the expression above is not far from a formulation that involves operators T_{W_N} and T_W applied to function ξ. Notice that the presence of the variable x inside the dependencies of ξ alters the action of the operator T_W. Thus, we must recast function ξ in a form that satisfies the requirements of the integral operator at hand.
Consider the decomposition:

$$\xi(x, x_*, s) = \bar{\xi}(x_*, s) + \delta\xi(x, x_*, s). \tag{4.21}$$

It is understood that:

$$\begin{cases} \bar{\xi}(x_*, s) = \displaystyle\int_0^1 \xi(x, x_*, s)\, dx \\ \displaystyle\int_0^1 \delta\xi(x, x_*, s)\, dx = 0. \end{cases}$$

Furthermore, recalling (4.14), we can infer that:

$$\begin{cases} |\xi(x, x_*, s)| \leq 2\mathrm{C} \\ |\bar{\xi}(x_*, s)| \leq \displaystyle\int_0^1 |\xi(x, x_*, s)|\, dx \leq 2\mathrm{C} \\ |\delta\xi(x, x_*, s)| = |\xi(x, x_*, s) - \bar{\xi}(x_*, s)| \leq 4\mathrm{C}. \end{cases}$$

Substituting this decomposition in the expression for Term ② we have:

$$\begin{aligned} ② &= \left| \int_0^1 \int_0^1 [W_N(x, x_*) - W(x, x_*)] \left[\bar{\xi}(x_*, s) + \delta\xi(x, x_*, s)\right] dx dx_* \right| \\ &\leq \left| \int_0^1 (T_{W_N} - T_W)\bar{\xi}(x_*, s) dx \right| + \left| \underbrace{\int_0^1 \int_0^1 [W_N(x, x_*) - W(x, x_*)] \delta\xi(x, x_*, s) dx dx_*}_{:=\mathrm{R}(x, x_*, s)} \right|. \end{aligned}$$

Exploiting the bound on the fluctuation term, we can estimate the residual R with the Lebesgue L^1-norm of the difference between W_N and W:

$$|\mathrm{R}(x, x_*, s)| \leq 4\mathrm{C} \int_0^1 \int_0^1 \left| W_N(x, x_*) - W(x, x_*) \right| dx dx_* = 4\mathrm{C} \|W_N - W\|_{L^1([0,1]^2)}. \tag{4.22}$$

Thus the final form of Term ②'s estimate becomes:

$$\textcircled{2} \leq \|T_{W_N} - T_W\|_{2,2}\|\bar{\xi}(\cdot,s)\|_{L^2([0,1])} + 4\mathrm{C}\|W_N - W\|_{L^1([0,1]^2)}. \tag{4.23}$$

It is crucial to observe that the validity of this estimate is contingent upon the finiteness of $\|\bar{\xi}(\cdot,s)\|_{L^2([0,1])}$. Indeed:

$$\begin{aligned}\|\bar{\xi}(\cdot,s)\|^2_{L^2([0,1])} &= \int_0^1 \left| \int_0^1 \left(\int_{\mathcal{O}} \int_{\mathcal{O}} (\Phi(y,v') - \Phi(y,v)) f_N(y,v,s) f_N(x_*,v_*,s) dv dv_* \right) dy \right|^2 dx_* \\ &\leq 4\mathrm{C}^2 < +\infty.\end{aligned}$$

In the end, we obtain the following estimate for Term ②:

$$\textcircled{2} \leq 2\mathrm{C}\left(\|T_{W_N} - T_W\|_{2,2} + 2\|W_N - W\|_{L^1([0,1]^2)} \right) \tag{4.24}$$

Applying the inequality from Theorem 3.3.1, we obtain a more refined estimate of Term ② that finally introduces the Cut Norm into the formulation:

$$\textcircled{2} \leq 2\mathrm{C}\left(\tilde{\mathrm{C}}\|W_N - W\|_{\square}^{\frac{1}{2}} + 2\|W_N - W\|_{L^1([0,1]^2)} \right). \tag{4.25}$$

In spite of this result, we can apply once again Grönwall's inequality and the final estimate takes the following form:

(4.26)
$$\begin{cases} \mathcal{W}_1(f_N(t), f(t)) \leq e^{2\tilde{k}t}\Big[\mathcal{W}_1(f_N(0), f(0)) + \mathrm{A}(t)\Big(\tilde{\mathrm{C}}\|W_N - W\|_{\square}^{\frac{1}{2}} + 2\|W_N - W\|_{L^1([0,1]^2)}\Big)\Big] \\ \text{where:} \quad A(t) = 2\mathrm{C}t, \quad \tilde{k} := \max(2\mathrm{C}\mathrm{L}_W, L_\Psi), \end{cases}$$

where we have exploited once more the equivalence between the operator norm $\|\cdot\|_{2,2}$ and the cut norm $\|\cdot\|_{\square}$, proved in Theorem 3.3.1.
Taking the $\sup_{t\in[0,T]}$ operator we obtain the following time-uniform estimate:

(4.27)
$$\begin{cases} \sup\limits_{t\in[0,T]} \mathcal{W}_1(f_N(t), f(t)) \leq e^{2\tilde{k}T}\Big[\mathcal{W}_1(f_N(0), f(0)) + \mathrm{A}(T)\Big(\tilde{\mathrm{C}}\|W_N - W\|_{\square}^{\frac{1}{2}} + 2\|W_N - W\|_{L^1([0,1]^2)}\Big)\Big], \\ \text{where:} \quad A(T) = 2\mathrm{C}T, \quad \tilde{k} := \max(2\mathrm{C}\mathrm{L}_W, L_\Psi). \end{cases}$$

Remark 4.4.4. *It is worth noting that convergence in the Lebesgue L^1-norm can be guaranteed by adopting an alternative construction for the discrete graphon W_N. If we assume the limit object W is already known and well-defined, W_N can be defined as a direct sampling of W evaluated at the representative points X_i, X_j within the partition of the unit interval* [0,1]*:*

$$W_N(x, x_*) := \sum_{i=1}^{N}\sum_{j=1}^{N} W(X_i, X_j)\chi_{I_i}(x)\chi_{I_j}(x_*).$$

This approach, supported by works such as [11, Proposition 4], significantly reduces the analytical requirements for convergence. However, it fundamentally alters the modelling interpretation of W_N, as it sacrifices the direct link to the adjacency matrix of the underlying empirical graph. While analytically convenient, the core results of this thesis rely on the definition of W_N derived strictly from the graph structure, as established in Chapter 3, to preserve the rigorous connection between the finite agent system and the continuous limit.

4.4.3 Convergence in the Cut Norm (Third Result)

Although the Lebesgue L^1-norm is generally stronger than the Cut Norm, it is possible to bound the former in terms of the latter by invoking a result from [5].

Proposition 4.4.1 (L^1 bound)**.** *Let $W \in L^1([0,1]^2)$ be a graphon. Then the following inequality holds:*

$$\|W\|_{L^1([0,1]^2)} \leq \sqrt{2N}\|W\|_{\square},$$

where N denotes the number of nodes in the associated discrete structure.

This result allows us to fully realize the goal of establishing convergence estimates relying solely on the Cut Norm, provided we impose specific constraints on the convergence rate, with respect to such norm, of the discrete graphon to its continuous limit. Indeed, revisiting the estimate for term ② in (4.25) and applying Proposition 4.4.1, we obtain:

$$② \leq 2\mathrm{C}\left(\tilde{\mathrm{C}}\|W_N - W\|_{\square}^{\frac{1}{2}} + 2\sqrt{2N}\|W_N - W\|_{\square}\right). \tag{4.28}$$

Let us define the error parameter $\epsilon := \|W_N - W\|_{\square}^{\frac{1}{2}}$ and assume a convergence rate of the form $\epsilon \sim N^{-\alpha}$ for some $\alpha > 0$. Substituting this scaling into the inequality yields:

$$a_1\epsilon + a_2\sqrt{N}\epsilon^2 \sim a_1 N^{-\alpha} + a_2 N^{-2\alpha+\frac{1}{2}},$$

where $a_1 = 2\mathrm{C}\tilde{\mathrm{C}}$ and $a_2 = 4\mathrm{C}\sqrt{2}$. To ensure that the error vanishes as $N \to \infty$, both terms must go to zero, that is to require:

$$\alpha > 0 \quad \text{and} \quad 2\alpha - \frac{1}{2} > 0 \implies \alpha > \frac{1}{4}.$$

We conclude that the least convergence rate admissible is $\|W_N - W\|_{\square} = \mathcal{O}(N^{-2\alpha})$ (i.e., an error decay faster than $1/\sqrt{N}$ is necessary to guarantee that the discrete equation correctly converges to the continuous one, in the limit $N \to \infty$).

Owing to the additional hypothesis on the rate of convergence of W_N with respect to the cut norm, the final estimate becomes:

(4.29)
$$\begin{cases} \mathcal{W}_1(f_N(t), f(t)) \leq e^{2\tilde{k}t}\Big[\mathcal{W}_1(f_N(0), f(0)) + \mathrm{A}(t)\Big(\tilde{\mathrm{C}}\|W_N - W\|_{\square}^{\frac{1}{2}} + 2\sqrt{2N}\|W_N - W\|_{\square}\Big)\Big] \\ \text{where:} \quad A(t) = 2\mathrm{C}t, \quad \tilde{k} := \max(2\mathrm{CL}_W, L_\Psi). \end{cases}$$

Taking the $\sup_{t\in[0,T]}$ operator one last time we retrieve:

(4.30)
$$\begin{cases} \sup\limits_{t\in[0,T]} \mathcal{W}_1(f_N(t), f(t)) \leq e^{2\tilde{k}T}\Big[\mathcal{W}_1(f_N(0), f(0)) + \mathrm{A}(T)\Big(\tilde{\mathrm{C}}\|W_N - W\|_{\square}^{\frac{1}{2}} + 2\sqrt{2N}\|W_N - W\|_{\square}\Big)\Big], \\ \text{where:} \quad A(T) = 2\mathrm{C}T, \quad \tilde{k} := \max(2\mathrm{CL}_W, L_\Psi). \end{cases}$$

4.5 Consistency with Established Kinetic Models

The model derived and rigorously justified is not only of academic relevance but it is a powerful tool in that it is able to reproduce interaction models from other pieces of literature. For instance, consider the work by Frasca et al. [11] and their continuous model indicated as (3) and reported below:

$$\frac{\partial}{\partial t}u(x,t) = \int_0^1 W(x,x_*)\Big[u(x_*,t) - u(x,t)\Big]dx_*, \tag{4.31}$$

with initial condition $u(x,0) = g(x)$.
The following considerations are made:

1. Let us consider linear, symmetric interactions, with $v' = v + \gamma(v_* - v)$, with $\gamma > 0$ a given scalar quantity. Moreover, let us observe that the chosen coefficients are deterministic and satisfy (4.4);
2. $u(x,t) := \int_0^1 vf(x,v,t)dv$ is defined as the average opinion of point $x \in [0,1]$ a time t;

These observations lead to the conclusions below:

- From 1. we have $\frac{1}{2}\langle \dots \rangle = \langle \Phi(x,v') - \Phi(x,v)\rangle$;
- Also from 1. we conclude that no stochasticity is present. Therefore:

$$\langle \Phi(x,v') - \Phi(x,v)\rangle = \Phi(x,v') - \Phi(x,v).$$

Substituting $\Phi(x,v) = \varphi(x)v$ in Equation (4.12) we get:

$$\frac{d}{dt}\int_0^1 \varphi(x)\underbrace{\int_{\mathcal{O}} vf(x,v,t)dv}_{:=u(x,t)}dx = \iint_{[0,1]^2} W(x,x_*)\varphi(x)\iint_{\mathcal{O}^2}\underbrace{\Big[v' - v\Big]}_{=\gamma(v_*-v)} f(x,v,t)f(x_*,v_*,t)dvdv_*dxdx_*.$$

Let us observe that the inner integrals on the right-hand side can be reformulated as:

$$\begin{aligned}
&\iint_{\mathcal{O}^2} \gamma(v_* - v) f(x,v,t) f(x_*,v_*,t) dv dv_* \\
&\quad = \gamma \iint_{\mathcal{O}^2} \Big[v_* f(x_*,v_*,t) f(x,v,t) - v f(x,v,t) f(x_*,v_*,t) \Big] \\
&\quad = \gamma \underbrace{\int_{\mathcal{O}} f(x,v,t) dv}_{=1} \underbrace{\int_{\mathcal{O}} v_* f(x_*,v_*,t) dv_*}_{:=u(x_*,t)} - \gamma \int_{\mathcal{O}} f(x_*,v_*,t) dv_* \int_{\mathcal{O}} v f(x,v,t) dv \\
&\quad = \gamma \Big[u(x_*,t) - u(x,t) \Big].
\end{aligned}$$

Substituting above:

(4.32)
$$\frac{d}{dt} \int_0^1 \varphi(x) u(x,t) dx = \int_0^1 \varphi(x) \left(\gamma \int_0^1 W(x,x_*) \Big[u(x_*,t) - u(x,t) \Big] dx_* \right) dx, \quad \forall \varphi \in \mathrm{Lip}_1([0,1]),$$

which is exactly the weak formulation of Equation (4.31), up to a multiplicative factor γ.

4.5.1 Nearest Neighbours Interactions

Let us consider Equation (4.31). Assuming that interactions are only allowed between close agents, let us consider the following interaction kernel:

$$W(x,x_*) = \chi(|x - x*| \leq R),$$

where R is a parameter such that $0 < R \ll 1$. Owing to these considerations, it is possible to expand in Taylor's series the difference $u(x_*,t) - u(x,t)$. By truncating the expansion at the second order we get:

$$u(x_*,t) - u(x,t) \approx \frac{\partial u}{\partial x}(x,t)\,(x - x_*) + \frac{1}{2} \frac{\partial^2 u}{\partial x^2}(x,t)(x - x_*)^2.$$

Substituting in (4.31):

$$\begin{aligned}
\frac{\partial u}{\partial t} &= \gamma \int_0^1 \chi(|x - x_*| \leq R) \Big[\frac{\partial u}{\partial x}(x,t)\,(x - x_*) + \frac{1}{2} \frac{\partial^2 u}{\partial x^2} (x - x_*)^2 \Big] dx_* \\
&= \gamma \int_0^1 \chi(|x - x_*| \leq R)\,(x - x_*)\,dx_* \frac{\partial u}{\partial x}(x,t) + \frac{\gamma}{2} \int_0^1 \chi(|x - x_*| \leq R)\,(x - x_*)^2\,dx_* \frac{\partial^2 u}{\partial x^2}(x,t) \\
&= \mathrm{A}_R(x) \frac{\partial u}{\partial x}(x,t) + \mathrm{B}_R(x) \frac{\partial^2 u}{\partial x^2}(x,t),
\end{aligned}$$

where:

$$\begin{cases}
\mathrm{A}_R(x) = \gamma \displaystyle\int_0^1 \chi(|x - x_*| \leq R)\,(x - x_*)\,dx_* \\
\mathrm{B}_R(x) = \dfrac{\gamma}{2} \displaystyle\int_0^1 \chi(|x - x_*| \leq R)\,(x - x_*)^2\,dx_*.
\end{cases}$$

The computation of these coefficients is strongly influenced by the presence of the indicator function $\chi(|x - x_*| \leq R)$. The variable of interest is $x_* \in [0,1] \cap [x - R, x + R]$, where $x \in [0,1]$. Thus, owing to the variability of parameter R the coefficients will be defined case by case.

1. Case $[x - R, x + R] \subseteq [0,1]$, which is verified when $x - R \geq 0 \ \wedge \ x + R \leq 1$. We have:

$$\begin{aligned} \mathrm{A}_R(x) &= \gamma \int_{x-R}^{x+R} (x - x_*) dx_* = 0 \\ \mathrm{B}_R(x) &= \frac{\gamma}{2} \int_{x-R}^{x+R} (x - x_*)^2 dx_* = \frac{\gamma}{3} R^3; \end{aligned}$$

2. Case $[0,1] \subseteq [x - R, x + R]$, which is verified when $x - R \leq 0 \ \wedge \ x + R \geq 1$. We have:

$$\begin{aligned} \mathrm{A}_R(x) &= \gamma \int_{0}^{1} (x - x_*) dx_* = \gamma (x - \frac{1}{2}) \\ \mathrm{B}_R(x) &= \frac{\gamma}{2} \int_{0}^{1} (x - x_*)^2 dx_* = \frac{\gamma}{6} (3x^2 - 3x + 1); \end{aligned}$$

3. Case of left partial overlap, which is verified when: $x - R \leq 0 \ \wedge \ x + R \leq 1$. We have:

$$\begin{aligned} \mathrm{A}_R(x) &= \gamma \int_{0}^{x+R} (x - x_*) dx_* = \frac{\gamma}{2} (x - R)(x + R) \\ \mathrm{B}_R(x) &= \frac{\gamma}{2} \int_{0}^{x+R} (x - x_*)^2 dx_* = \frac{\gamma}{6} (x^3 + R^3); \end{aligned}$$

4. Case right partial overlap, which is verified when $x - R \geq 0 \ \wedge \ x + R \geq 1$. We have:

$$\begin{aligned} \mathrm{A}_R(x) &= \gamma \int_{x-R}^{1} (x - x_*) dx_* = -\frac{\gamma}{2} (x - R - 1)(x + R - 1) \\ \mathrm{B}_R(x) &= \frac{\gamma}{2} \int_{x-R}^{1} (x - x_*)^2 dx_* = \frac{\gamma}{6} \left(R^3 - (x - 1)^3 \right) \end{aligned}$$

5. Case of non-existent overlap. Such case is not allowed due to the constraint $x \in [0,1]$.

Remark 4.5.1. *It is possible to refine the cases considered above by imposing the hypothesis $R \ll 1$. Specifically, we assume $R \leq \frac{1}{2}$. Consequently, Case 2 does not occur, and the remaining cases, ordered according to $x \in [0,1]$, allow the coefficients $\mathrm{A}_R(x)$ and $\mathrm{B}_R(x)$ to be rewritten as follows:*

$$\mathrm{A}_R(x) = \begin{cases} \frac{\gamma}{2}(x^2 - R^2) & \text{for } x \leq R \\ 0 & \text{for } R \leq x \leq 1 - R \\ -\frac{\gamma}{2}\left((x-1)^2 - R^2\right) & \text{for } 1 - R \leq x \leq 1. \end{cases}$$

$$\mathrm{B}_R(x) = \begin{cases} \frac{\gamma}{6}(x^3 + R^3) & \text{for } x \leq R \\ \frac{\gamma}{3}R^3 & \text{for } R \leq x \leq 1 - R \\ \frac{\gamma}{6}\left(R^3 - (x-1)^3\right) & \text{for } 1 - R \leq x \leq 1. \end{cases}$$

Remark 4.5.2 (Physical Interpretation)**.** *This is, therefore, a non-stationary parabolic diffusion-transport equation with variable coefficients. This implies that, in a neighbourhood of the point* $(x, x_*) \in [0,1]^2$*, the time evolution of the mean opinion* $u(x,t)$ *is governed by two factors: the first is a convection process with non-constant velocity* $\mathrm{A}_R(x)$*; the second is a diffusion process with non-constant coefficient* $\mathrm{B}_R(x)$*. The term* $\mathrm{A}_R(x)\frac{\partial u}{\partial x}$ *describes the opinion drift process, where* $\mathrm{A}_R(x)$ *represents the drift velocity. Its dependence on the spatial coordinate* x *is a specific feature of the model, allowing for the analysis of scenarios where, for instance, the mean opinion is more susceptible to influence in certain cities than in others. The term* $\mathrm{B}_R(x)\frac{\partial^2 u}{\partial x^2}$ *becomes significant where the function* $u(x,t)$ *exhibits peaks, i.e., where the mean opinion is highly polarized. The role of this diffusion term is to smooth out these spatial discrepancies and to describe the rate (determined by the coefficient* $\mathrm{B}_R(x)$*) at which mean opinions mutually influence one another until consensus is reached. We observe that, for both the convective and diffusive terms, the parameter* R *appears in the numerator raised to a power (quadratic for convection and cubic for diffusion). This implies that, within the limits of validity for the series expansion of the difference* $u(x_*,t) - u(x,t)$*, the larger the chosen neighbourhood, the more the mean opinion tends to disperse in space.*

Chapter 5

Study of the Statistical Moments

The degree of freedom represented by the choice of $\Phi(x, v)$ in Equation (4.12) becomes useful in the study of statistical moments of f. Specifically, if we take $\Phi(x, v) = \varphi(x)\, v^n$ we can define the n-th order statistical moment of f as:

$$\mathrm{M}_n(x, t) := \int_{\mathcal{O}} v^n f(x, v, t)\, dv. \tag{5.1}$$

By choosing suitable indices, we will be able to gather information on the Zeroth Order Moment (i.e. information about the time evolution of the system's mass), the Mean Opinion M_1, the Energy of the system M_2 and its Variance $(\mathrm{Var}(f))\,(x, t) := \mathrm{M}_2(x, t) - \mathrm{M}_1^2(x, t)$.

5.1 Time Evolution of the n-th Order Moment

Substituting $\Phi(x, v) = \varphi(x)v^n$ into Equation (4.12) allows us to obtain:

$$\begin{aligned}\frac{d}{dt}\int_0^1 \varphi(x) \int_{\mathcal{O}} v^n f(t) dv dx = \iint_{[0,1]^2} \varphi(x) W(x, x_*) \\ \times \iint_{\mathcal{O}^2} \langle (pv + qv_*)^n - v^n \rangle f(t) f^*(t) dv dv_* dx dx_*.\end{aligned}$$

Recalling the formula for the binomial expansion, we can rewrite the difference inside the angle brackets as:

$$\langle (pv + qv_*)^n - v^n \rangle = \sum_{k=0}^{n} \binom{n}{k} \langle p^k q^{n-k} \rangle v^k v_*^{n-k} - v^n,$$

thus obtaining:

$$
\begin{aligned}
&= \iint_{[0,1]^2} \varphi(x) W(x,x_*) \iint_{\mathcal{O}^2} \left[\sum_{k=0}^{n} \binom{n}{k} \langle p^k q^{n-k} \rangle v^k v_*^{n-k} - v^n \right] f(t) f^*(t) dv dv_* dx dx_* \\
&= \iint_{[0,1]^2} \varphi(x) W(x,x_*) \left[\sum_{k=0}^{n} \binom{n}{k} \langle p^k q^{n-k} \rangle \int_{\mathcal{O}} v^k f(t)\, dv \int_{\mathcal{O}} v_*^{n-k} f^*(t)\, dv_* - \mathrm{M}_n(x,t) \right] dx\, dx_* \\
&= \sum_{k=0}^{n} \binom{n}{k} \langle p^k q^{n-k} \rangle \iint_{[0,1]^2} \varphi(x) W(x,x_*) \mathrm{M}_k(x,t) \mathrm{M}_{n-k}(x_*,t) dx dx_* - \iint_{[0,1]^2} \varphi(x) W(x,x_*) \mathrm{M}_n(x,t) dx dx_* \\
&= \sum_{k=0}^{n} \binom{n}{k} \langle p^k q^{n-k} \rangle \int_0^1 \varphi(x) \mathrm{M}_k(x,t) \left(T_W \mathrm{M}_{n-k}(\cdot,t) \right)(x) dx - \int_0^1 \varphi(x) \mathrm{M}_n(x,t) \mathrm{d}_W(x) dx.
\end{aligned}
$$

Finally we arrive to:

$$
\begin{aligned}
\frac{d}{dt} \int_0^1 \varphi(x) \mathrm{M}_n(x,t) dx = \int_0^1 \varphi(x) \Bigg[&\sum_{k=0}^{n} \binom{n}{k} \langle p^k q^{n-k} \rangle \mathrm{M}_k(x,t) \left(T_W \mathrm{M}_{n-k}(\cdot,t) \right)(x) \\
&- \mathrm{M}_n(x,t) \mathrm{d}_W(x) \Bigg] dx, \ \forall \varphi \in \mathrm{Lip}_1([0,1]),
\end{aligned}
$$

whence the strong form:

$$
\frac{\partial \mathrm{M}_n}{\partial t}(x,t) = \sum_{k=0}^{n} \binom{n}{k} \langle p^k q^{n-k} \rangle \mathrm{M}_k(x,t) \left(T_W \mathrm{M}_{n-k}(\cdot,t) \right)(x) - \mathrm{M}_n(x,t) \mathrm{d}_W(x). \tag{5.2}
$$

Notice that the role of M_n at the right-hand side can be further emphasized by extracting the terms for $k = 0$ and $k = n$ from the sum above:

$$
\begin{aligned}
\frac{\partial \mathrm{M}_n}{\partial t}(x,t) = \langle q^n \rangle \mathrm{M}_0(x,t) \left(T_W \mathrm{M}_n(\cdot,t) \right)(x) + \langle p^n \rangle \mathrm{M}_n(x,t) \left(T_W \mathrm{M}_0(\cdot,t) \right)(x) - \mathrm{M}_n(x,t) \mathrm{d}_W(x) \\
+ \sum_{k=1}^{n-1} \binom{n}{k} \langle p^k q^{n-k} \rangle \mathrm{M}_k(x,t) \left(T_W \mathrm{M}_{n-k}(\cdot,t) \right)(x), \quad n \geq 1.
\end{aligned}
$$

It is important to stress that this form is only valid when $n \geq 1$. For the case $n = 0$ we refer to Section 5.1.1.

Remark 5.1.1 (Retrieval of the Spatially Homogeneous Moment Equations)**.** *It is instructive to consider the limiting case where the network structure is absent, corresponding to the mean-field assumption $W(x,x_*) \equiv 1$. In this regime, interactions occur with uniform probability across the entire domain, and we expect to recover the classical moment equations for spatially homogeneous opinion dynamics.*

Starting from the general evolution Equation (5.2) for the local moment $\mathrm{M}_n(x,t)$, we integrate both sides over the spatial domain $[0,1]$. Under the assumption $W \equiv 1$, the spatial integrals on the right-hand side decouple:

$$\int_0^1 \mathrm{M}_k(x,t)\int_0^1 \mathrm{M}_{n-k}(x_*,t)\,dx_*\,dx = \left(\int_0^1 \mathrm{M}_k(x,t)\,dx\right)\left(\int_0^1 \mathrm{M}_{n-k}(x_*,t)\,dx_*\right).$$

Defining the spatially homogeneous n-th order moment $\mathrm{m}_n(t)$ *as the spatial average of the local moment:*

$$\mathrm{m}_n(t) := \int_0^1 \mathrm{M}_n(x,t)\,dx,$$

the integration of the governing equation yields:

$$\frac{d\mathrm{m}_n}{dt}(t) = \sum_{k=0}^{n}\binom{n}{k}\langle p^k q^{n-k}\rangle\,\mathrm{m}_k(t)\mathrm{m}_{n-k}(t) - \mathrm{m}_n(t). \tag{5.3}$$

Equation (5.3) is recognized as the standard moments' equation for spatially homogeneous kinetic models of opinion dynamics (see, e.g., [9]), confirming that the proposed graphon framework is a consistent generalization of the classical theory.

5.1.1 Conservation of the Total Mass – Zeroth Order Moment

Let now $n = 0$. Substituting this value into Equation (5.2) we obtain:

$$\frac{\partial \mathrm{M}_0}{\partial t}(x,t) = \mathrm{M}_0(x,t)\Big[\left(T_W \mathrm{M}_0(\cdot,t)\right)(x) - \mathrm{d}_W(x)\Big]. \tag{5.4}$$

Notice that $\mathrm{M}_0(x,t)$ can be reformulated in terms of the marginal of f, with respect to the opinion variable. Indeed:

$$\mathrm{M}_0(x,t) = \int_{\mathcal{O}} f(x,v,t)\,dv = F(x,t).$$

In Remark 4.4.2 we showed that the discrete counter part $F_N(x,t) \equiv 1$, $\forall x \in [0,1]$, $\forall t \geq 0$. This feature preserves itself in the limit $N \to \infty$, thus implying that:

$$\mathrm{M}_0(x,t) = F(x,t) \equiv 1.$$

Substituting this information in Equation (5.4), and noticing that:

$$\left(T_W\,1\right)(x) = \int_0^1 W(x,x_*)\,dx_* = \mathrm{d}_W(x),$$

we can conclude that, by construction, the conservation in time of the total mass of the system is guaranteed.
As stated in Remark 5.1.1, either by choosing $n = 0$ in Equation (5.3) or letting $W \equiv 1$ and substituting this information in Equation (5.4), it is possible to retrieve the equation for the time evolution of the mass of the system in the spatially homogeneous case:

$$\frac{d\mathrm{m}_0}{dt}(t) = \mathrm{m}_0(t)\Big[\mathrm{m}_0(t) - 1\Big]. \tag{5.5}$$

5.1.2 Average Opinion – First Order Moment

Let $n = 1$. The first order moment with respect to variable v represents the mean opinion of the generic agent $x \in [0,1]$ at time $t > 0$. By substituting this value for n in Equation (5.2) we get:

$$\frac{\partial \mathrm{M}_1}{\partial t}(x,t) = \langle q \rangle \left(T_W \mathrm{M}_1(\cdot,t)\right)(x) + \langle p-1 \rangle \mathrm{d}_W(x)\mathrm{M}_1(x,t), \tag{5.6}$$

where we have taken $\mathrm{M}_0(x,t) = 1$, as previously demonstrated.
As already done for Equation (5.5), the time evolution equation for the mean opinion in the homogeneous case reads as follows:

$$\frac{d\mathrm{m}_1}{dt}(t) = \langle p+q-1 \rangle \mathrm{m}_1(t). \tag{5.7}$$

A comparison between the general evolution Equation (5.6) and its homogeneous counterpart (5.7) reveals the explicit dependence of the dynamics on the network topology. The general equation is governed by the graphon W through two distinct mechanisms: it shapes the consensus dynamics via the integral operator T_W (representing weighted averaging of opinions), and it modulates the local interaction rate via the degree function $\mathrm{d}_W(x)$ (representing the connectivity intensity). In the spatially homogeneous limit ($W \equiv 1$), these topological constraints vanish. The connectivity becomes uniform, implying $\mathrm{d}_W(x) = 1$, $\forall x \in [0,1]$, while the operator T_W reduces to a simple global integration over $[0,1]$. This reduction confirms that in the absence of graph structure, the evolution is driven purely by a mean-field interaction where all agents influence each other equally, independent of their position.

5.1.3 Energy of the System – Second Order Moment

The second order moment represents the Energy of the system. It is usually good practice to make sure that it does not diverge by imposing suitable conditions on the coefficients p, q. Let $n = 2$ and substitute once again in Equation (5.2). We obtain:

$$\begin{aligned}\frac{\partial \mathrm{M}_2}{\partial t}(x,t) = {} & \langle q^2 \rangle \left(T_W \mathrm{M}_2(\cdot,t)\right)(x) + 2\langle pq \rangle \mathrm{M}_1(x,t)\left(T_W \mathrm{M}_1(\cdot,t)\right)(x) \\ & + \langle p^2 - 1 \rangle \mathrm{M}_2(x,t)\mathrm{d}_W(x).\end{aligned} \tag{5.8}$$

The inhomogeneous case depicted above does not allow for a useful analysis due to its intricate structure. However, considering the homogeneous case (i.e. Equation (5.3) with $n = 2$) we obtain a more tractable formulation that allows us to retrieve a set of conditions to impose on the coefficients in order to guarantee the well-posedness of the system in terms of its Energy. Indeed, starting from:

$$\frac{d\mathrm{m}_2}{dt}(t) = \langle p^2 + q^2 - 1\rangle \mathrm{m}_2(t) + 2\langle pq\rangle \mathrm{m}_1^2(t) \tag{5.9}$$

we first notice that the condition $\langle p + q\rangle = 1$ substituted in Equation (5.7) guarantees that $\mathrm{m}_1(t) \equiv \mathrm{m}_{1,0}, \forall t \geq 0$. Thus, we may recast Equation (5.9) in the following, more convenient form:

$$\frac{d\mathrm{m}_2}{dt}(t) = \alpha \mathrm{m}_2(t) + \beta, \tag{5.10}$$

where $\alpha := \langle p^2 + q^2 - 1\rangle$ and $\beta := 2\langle pq\rangle \mathrm{m}_{1,0}^2$. Its general solution reads as follows:

$$\mathrm{m}_2(t) = \left(-\frac{\beta}{\alpha} e^{-\alpha t} + \mathrm{c}\right) e^{\alpha t},$$

where c is the integration constant. It is clear that we must have $\alpha = \langle p^2 + q^2\rangle - 1 < 0$ so that $\mathrm{m}_2(t)$ does not diverge, as $t \to +\infty$.
In conclusion, the set of conditions:

$$\begin{cases} \langle p^2 + q^2\rangle < 1 \\ \langle p + q\rangle = 1 \end{cases}$$

is sufficient to ascertain that $\mathrm{m}_2(t)$, as $t \to +\infty$, approaches some value $\mathrm{m}_2^\infty \in (0, E),\ E < +\infty$, in accordance with its physical meaning.

5.2 Existence of Asymptotic States

A common task in kinetic theories is to determine whether the system admits an asymptotic state, identified through its distribution function f^∞. Such matter is particularly case-dependent and its resolution can become quite cumbersome.
One way around this issue is to rest content of studying the asymptotic trends of the equilibrium points of equations such as Equation (5.6) and Equation (5.8). Let us indicate the asymptotic state of the average opinion as $\mathrm{M}_1^\infty(x)$, and the asymptotic state of the energy of the system as $\mathrm{M}_2^\infty(x)$.
We first focus on analysing the existence of the opinion's equilibrium states.

5.2.1 Existence and Computation of Average Opinion Equilibrium States

The asymptotic opinion state M_1^∞ must satisfy the following equation:

$$\langle q\rangle \left(T_W \mathrm{M}_1^\infty\right)(x) + \langle p - 1\rangle \mathrm{d}_W(x) \mathrm{M}_1^\infty(x) = 0, \tag{5.11}$$

Firstly, let us notice that, by manipulating its terms, we may rewrite such equation in the following manner:

$$\begin{aligned}\mathrm{M}_1^{\infty}(x) &= \frac{\langle q\rangle}{\langle 1-p\rangle}\frac{1}{\int_0^1 W(x,x_*)dx_*}\int_0^1 W(x,x_*)\mathrm{M}_1^{\infty}(x_*)dx_* \\ &= \int_0^1 K_{p,q}(x,x_*)\mathrm{M}_1^{\infty}(x_*)dx_* \\ &= \left(T_{K_{p,q}}\mathrm{M}_1^{\infty}\right)(x), \quad \forall t \geq 0,\end{aligned}$$

showing that, regardless of its structure, M_1^{∞} is an eigenfunction of operator $T_{K_{p,q}}$ with eigenvalue $\lambda = 1$.
For the sake of argument, let us consider a constant initial average opinion $\mathrm{M}_1(x,0) \equiv c \in \mathbb{R}$. We shall see that, under already given assumptions, this choice will lead to $\mathrm{M}_1^{\infty}(x) \equiv c$. Indeed, we can instantly notice that, by substituting this information in Equation (5.11), we get:

$$\langle q\rangle \mathrm{d}_W(x)c + \langle p-1\rangle \mathrm{d}_W(x)c = 0,$$

which simplifies to:

$$\langle p+q\rangle = 1,$$

assuming $\mathrm{d}_W(x) > 0$. Next, we verify that the absence of the spatial dependence at the initial time is preserved during the interaction process. Indeed, generically assuming that $\mathrm{M}_1(x,t) = \mathfrak{F}(t)$ and substituting into Equation (5.6) we obtain:

$$\begin{aligned}\frac{d}{dt}\mathfrak{F}(t) &= \langle q\rangle \mathrm{d}_W(x)\mathfrak{F}(t) + \langle p-1\rangle \mathrm{d}_W(x)\mathfrak{F}(t) \\ &= \langle p+q-1\rangle \mathrm{d}_W(x)\mathfrak{F}(t),\end{aligned}$$

which is equal to zero, due to condition $\langle p+q\rangle = 1$ being already satisfied when choosing $\mathrm{M}_1(x,0) \equiv c$. Therefore, an initial spatially homogeneous average opinion remains such, $\forall t \geq 0$, which leads to the conclusion $\mathrm{M}_1^{\infty}(x) \equiv c$.

Remark 5.2.1 (Connectivity of the network)**.** *If* $\mathrm{d}_W(x) = 0$*, for some* $x \in [0,1]$*, this would imply that the graph* $\mathcal{G}_N$ *contains an isolated node. As such, it does not contribute to the dynamics and can thus be removed, especially when considering the limit* $N \to \infty$*. Hence, it is reasonable enough to assume that no isolated node exists inside the graph* $\mathcal{G}_N$*, thus implying that* $\exists\, \delta > 0$ *such that* $\mathrm{d}_W(x) \geq \delta > 0$, $\forall x \in [0,1]$*. This results in:*

$$\frac{1}{\mathrm{d}_W(x)} \leq \frac{1}{\delta} := M.$$

Now, suppose we are interested in studying the asymptotic trend of the average opinion $\mathrm{M}_1(x,t)$. As we just demonstrated, $\mathrm{M}_1(x,t) \equiv c$ represents an equilibrium state, and therefore represents one solution to Equation (5.11). More specifically, any constant function is an eigenfunction of operator $T_{K_{p,q}}$ corresponding to the eigenvalue $\lambda = 1$. Mathematically, this confirms that constant functions correspond to equilibrium states. While this outcome is trivial, it demonstrates the consistency of the derived framework.

Given a generic equilibrium state $\mathrm{M}_1^\infty(x)$, it must satisfy the following relation:

$$\mathrm{M}_1^\infty(x) = \left(T_{K_{p,q}} \mathrm{M}_1^\infty\right)(x), \tag{5.12}$$

Thus, proving the existence of the solutions M_1^∞ to Equation (5.12) is equivalent to showing that the spectrum of operator $T_{K_{p,q}}$ contains the eigenvalue $\lambda = 1$.
Before continuing, let us give the following remark.

Remark 5.2.2. *Operator $T_{K_{p,q}}$ is well-defined as an operator from $L^2([0,1])$ into itself. Indeed, given a function $h \in L^2([0,1])$ we have:*

$$\begin{aligned}
\|T_{K_{p,q}} h\|^2_{L^2([0,1])} &= \int_0^1 \left| K_{p,q}(x, x_*) h(x_*) dx_* \right|^2 dx \\
&\leq \int_0^1 \left[\int_0^1 \left| K_{p,q}(x, x_*) \right|^2 dx_* \, \|h\|^2_{L^2([0,1])} \right] \\
&= \|h\|^2_{L^2([0,1])} \int_0^1 \int_0^1 \left| K_{p,q}(x, x_*) \right|^2 dx_* dx.
\end{aligned}$$

To address the last term, let us recall that:

$$K_{p,q}(x, x_*) = \frac{\langle q \rangle}{\langle 1 - p \rangle} \frac{W(x, x_*)}{\mathrm{d}_W(x)},$$

where $\mathrm{d}_W(x) = \int_0^1 W(x, x_*) dx_*$. Finally, exploiting the bound $W(x, x_*) \leq 1$ and $\frac{1}{\mathrm{d}_W(x)} \leq \frac{1}{\delta} := M$ we get:

$$\|T_{K_{p,q}} h\|_{L^2([0,1])} \leq M \frac{\langle q \rangle}{\langle 1 - p \rangle} \|h\|_{L^2([0,1])} < +\infty. \tag{5.13}$$

Lastly, in order to guarantee that operator $T_{K_{p,q}}$'s spectrum allows $\lambda = 1$ as one of its eigenvalues – i.e., there exist solutions to Equation (5.12) – we must provide upper and lower bounds on its spectral radius ρ. In this work, we only give an upper bound.
It is known that, given an operator T:

$$\sigma(T) = \{\lambda \in \mathbb{C} \,|\, |\lambda| \leq \rho(T)\},$$

where $\rho(T) \leq \|T\|_{2,2}$. Applying these results to operator $T_{K_{p,q}}$, from (5.13) we can see that:

$$\rho(T_{K_{p,q}}) \leq \|T_{K_{p,q}}\|_{2,2} = M \frac{\langle q \rangle}{\langle 1 - p \rangle} = M,$$

when $\langle p + q \rangle = 1$.

5.2.2 Existence and Computation of Energy Equilibrium States

Consider Equation (5.8). The asymptotic state M_2^∞ is such that:

$$\langle q^2\rangle \left(T_W \mathrm{M}_2^\infty\right)(x) + 2\langle pq\rangle \mathrm{M}_1^\infty(x) \left(T_W \mathrm{M}_1^\infty\right)(x) + \langle p^2-1\rangle \mathrm{M}_2^\infty(x) \mathrm{d}_W(x) = 0. \tag{5.14}$$

To obtain an implicit equation for M_2^∞, we can expand and rearrange the terms in the equation above to obtain the following:

$$\begin{aligned}\frac{\langle q^2\rangle}{\langle 1-p^2\rangle}\frac{1}{\mathrm{d}_W(x)}\int_0^1 W(x,x_*)\mathrm{M}_2^\infty(x_*)\,dx_* = \mathrm{M}_2^\infty(x) \\ - \frac{1}{\langle 1-p^2\rangle}\frac{1}{\mathrm{d}_W(x)}\left(S_{p,q}(\mathrm{M}_1^\infty,\mathrm{M}_1^\infty)\right)(x),\end{aligned} \tag{5.15}$$

where:

$$\left(S_{p,q}(\mathrm{M}_1^\infty,\mathrm{M}_1^\infty)\right)(x) = 2\langle pq\rangle \frac{\langle q\rangle}{\langle 1-p\rangle \mathrm{d}_W(x)} \int_0^1 W(x,x_*)\mathrm{M}_1^\infty(x_*)\,dx_* \int_0^1 W(x,y)\mathrm{M}_1^\infty(y)\,dy$$

is a new operator. Notice that it is well-posed as an operator from $L^2([0,1])\times L^2([0,1]) \to L^2([0,1])$, as long as $\mathrm{M}_1^\infty \in L^2([0,1])$. Indeed:

$$\begin{aligned}\|S_{p,q}(\mathrm{M}_1^\infty,\mathrm{M}_1^\infty)\|^2_{L^2([0,1])} &= 4\langle pq\rangle^2 \int_0^1 \left|\left(T_K \mathrm{M}_1^\infty\right)\left(T_W \mathrm{M}_1^\infty\right)\right|^2 dx \\ &\le 4\langle pq\rangle^2 M^2 \|\mathrm{M}_1^\infty\|^4_{L^2([0,1])}.\end{aligned}$$

The final expression becomes:

$$\left(T_{\tilde{K}_{p,q}}\mathrm{M}_2^\infty\right)(x) = \mathrm{M}_2^\infty - \frac{1}{\mathrm{d}_W(x)\langle 1-p^2\rangle}\left(S_{p,q}(\mathrm{M}_1^\infty,\mathrm{M}_1^\infty)\right)(x), \tag{5.16}$$

where $T_{\tilde{K}_{p,q}}$ is a newly defined operator with kernel:

$$\tilde{K}_{p,q}(x,x_*) := \frac{\langle q^2\rangle}{\langle 1-p^2\rangle}\frac{W(x,x_*)}{\mathrm{d}_W(x)}.$$

5.3 Consensus of Opinions

In the limit as $t \to +\infty$, under reasonable assumptions, interactions generally lead the system toward a stationary state. Such a configuration is an equilibrium, obtained analytically by imposing the time derivative of the statistical moments to be zero.

It is particularly interesting to analyse under which constraints a system of interacting agents reaches a *consensus* state. This regime is statistically characterized by a stationary distribution f^∞ that approaches a Dirac delta function centered at the mean opinion,

implying that all agents eventually share the same microscopic state. Mathematically, convergence to consensus is equivalent to the vanishing of the local variance:

$$\lim_{t\to+\infty}(\mathrm{Var}f^{\infty})(x,t)=0,\quad \forall x\in[0,1].$$

Using the definition of variance, this condition implies:

$$\mathrm{M}_2^{\infty}(x)-(\mathrm{M}_1^{\infty}(x))^2=0.$$

Note that this formulation is well-posed given the existence results for equilibrium points discussed in Sections 5.2.1 and 5.2.2.

Substituting the implicit expressions for M_1^{∞} and M_2^{∞} derived from Equation (5.11) and Equation (5.14), respectively, we obtain:

$$\frac{1}{\langle 1-p^2\rangle \mathrm{d}_W(x)}\left[\langle q^2\rangle\left(T_W\mathrm{M}_2^{\infty}\right)(x)+2\langle pq\rangle\frac{\langle q\rangle}{\langle 1-p\rangle \mathrm{d}_W(x)}\left(T_W\mathrm{M}_1^{\infty}\right)^2(x)\right]-\frac{\langle q\rangle^2}{\langle 1-p\rangle^2\mathrm{d}_W^2(x)}\left(T_W\mathrm{M}_1^{\infty}\right)^2(x)=0$$

After some algebra, we get to the final formulation:

$$\left(T_W\mathrm{M}_2^{\infty}\right)(x)-\frac{1}{\mathrm{d}_W(x)}\left[1-\frac{2\langle q\rangle\langle pq\rangle}{\langle q^2\rangle\langle 1-p\rangle}\right]\left(T_W\mathrm{M}_1^{\infty}\right)^2(x)=0 \tag{5.17}$$

Thus, when condition (5.17) is satisfied, the system will asymptotically reach consensus. The structure of this constraint highlights the explicit dependence on the network topology via the operator T_W and the degree function $\mathrm{d}_W(x)$. Unlike the classical spatially homogeneous case, where consensus conditions depend purely on interaction parameters, here the local connectivity plays a crucial role in determining whether a consensus state can be achieved or not.

Remark 5.3.1 (Recovery of the spatially homogeneous case)**.** *We notice that, by letting* $W\equiv 1$ *and using the definition* $\mathrm{m}_n^{\infty}:=\int_0^1\mathrm{M}_n^{\infty}(x)\,dx$*, for* $n=1,2$*, as the new unknown variable we recover the consensus condition for the spatially homogeneous case, whenever conditions* $\langle p+q\rangle=1$ *and* $\langle p^2+q^2\rangle<1$ *are satisfied. Indeed:*

$$\mathrm{m}_2^{\infty}\frac{\langle q^2\rangle}{\langle 1-p^2\rangle}+(\mathrm{m}_1^{\infty})^2\left[\frac{2\langle pq\rangle}{\langle 1-p^2\rangle}-1\right]=0 \tag{5.18}$$

Achieving consensus, i.e. imposing that the variance of the distribution vanishes, translates to requiring that $\mathrm{m}_2^{\infty}=(\mathrm{m}_1^{\infty})^2$*. Substituting in the expression above we finally obtain:*

$$\begin{aligned}&\langle q^2\rangle+2\langle pq\rangle=\langle 1-p^2\rangle\\ \Longrightarrow\ &\langle(p+q)^2\rangle=1,\end{aligned}$$

which is exactly the consensus condition for the homogeneous case, as it is shown by [9].

5.4 Ochrombel Simplification of the Sznajd Model

The Sznajd Model The Sznajd model is a very simple socio-physics model introduced at the beginning of this century. It is most commonly referred to as USDF – United we Stand, Divided we Fall. The model implements the phenomenon called Social Validation and thus extends the Ising spin model [1]. In other words, the model states that:

- Social Validation: when two contiguous agents agree, then also their neighbours start to agree with them;
- Discord Destruction: if the two proximal agents differ in their state, then also their neighbours will start to argue.

For simplicity, we can assume that each individual i can have one of two opinions, which are described as $+1$ and -1. The present model allows to reach either one of two states, namely complete consensus or stalemate, as simple Monte Carlo simulations show:

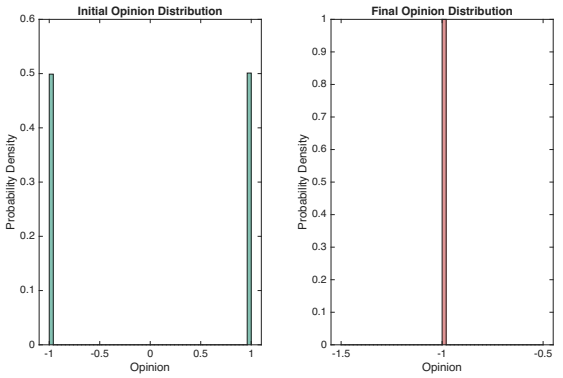

Figure 5.1. The Sznajd Model: Negative consensus

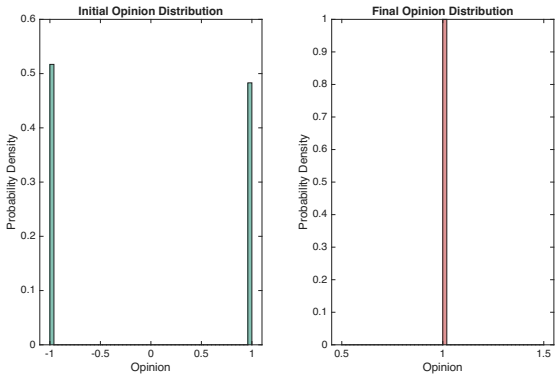

Figure 5.2. The Sznajd Model: Positive consensus

[1] The Ising Spin Model was originally designed to describe how magnets work. It was later employed to describe the interactions that can be modelled in a dichotomic manner.

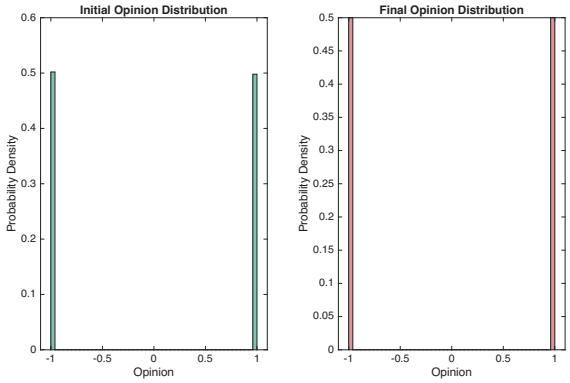

Figure 5.3. The Sznajd Model: Stalemate state

Written in formulas, the interaction laws read:

$$\begin{aligned}
&\text{Social Validation:} && S_i = S_{i+1} \Rightarrow S_{i-1} = S_i \quad \text{and } S_{i+1} = S_i \\
&\text{Discord Destruction:} && S_i = -S_{i+1} \Rightarrow S_{i-1} = S_{i+1} \text{ and } S_{i+2} = S_i.
\end{aligned}$$

Ochrombel Simplification In the Ochrombel simplification of the Sznajd model the interaction rules are:

$$\begin{cases} v' = v \\ v'_* = v \end{cases} \tag{5.19}$$

In other words, an interaction between two individuals leads to a post interaction state which is characterized by the total annihilation of one of the two pre-interaction states.

Remark 5.4.1. *Notice that these interaction rules can be derived from:*

$$\begin{cases} v' = pv + qv_* \\ v'_* = p_*v_* + q_*v \end{cases}$$

by taking $p = q_* = 1$ *and* $p_* = q = 0$.

Now, consider Equation (4.10) for non-symmetric interactions. In order to study how the statistical moments of f vary if compared to the general case, we can take $\Phi(x, v) = \varphi(x)v^n$. Recalling the definition of $\mathrm{M}_n(x, t)$ and substituting into the considered equation we obtain:

$$\begin{aligned}
\frac{d}{dt}\int_0^1\int_{\mathcal{O}} \varphi(x)v^n f(x,v,t)dvdx = \int_0^1\int_0^1 W(x,x_*)\int_{\mathcal{O}}\int_{\mathcal{O}} \frac{1}{2}\left[\varphi(x)v^n + \varphi(x_*)v^n - \varphi(x)v^n - \varphi(x_*)v_*^n\right] \\
\times f(x,v,t)f(x_*,v_*,t)dvdv_*dxdx_*
\end{aligned}$$

$$
\begin{aligned}
&= \int_0^1 \int_0^1 W(x,x_*)\varphi(x_*) \int_{\mathcal{O}}\int_{\mathcal{O}} \left[v^n - v_*^n\right] f(x,v,t) f(x_*,v_*,t) dv dv_* dx dx_* \\
&= \int_0^1 \int_0^1 W(x,x_*)\varphi(x_*) \frac{1}{2}\left[\int_{\mathcal{O}} v^n f(x,v,t) dv \int_{\mathcal{O}} f(x_*,v_*,t) dv_* - \int_{\mathcal{O}} f(x,v,t) dv \int_{\mathcal{O}} v_*^n f(x_*,v_*,t) dv_* \right] dx dx_* \\
&= \int_0^1 \int_0^1 W(x,x_*)\varphi(x_*) \frac{1}{2}\Big[\mathrm{M}_n(x,t) - \mathrm{M}_n(x_*,t) \Big] dx dx_* \\
&= \int_0^1 \int_0^1 W(x,x_*)\varphi(x) \frac{1}{2}\Big[\mathrm{M}_n(x_*,t) - \mathrm{M}_n(x,t) \Big] dx dx_* \\
&= \int_0^1 \varphi(x) \int_0^1 W(x,x_*) \frac{1}{2} \mathrm{M}_n(x_*,t) dx_* dx - \int_0^1 \varphi(x) \int_0^1 W(x,x_*) dx_* \frac{1}{2} \mathrm{M}_n(x,t) dx.
\end{aligned}
$$

Finally arriving at:

$$
\int_0^1 \varphi(x) \frac{\partial \mathrm{M}_n}{\partial t}(x,t) dx = \int_0^1 \varphi(x) \frac{1}{2}\left[\int_0^1 W(x,x_*) \mathrm{M}_n(x_*,t) dx_* - \int_0^1 W(x,x_*) dx_* \mathrm{M}_n(x,t) \right] dx,
$$

$\forall \varphi \in \mathrm{Lip}_1([0,1])$. The equation in its strong formulation reads:

$$
\frac{\partial \mathrm{M}_n}{\partial t}(x,t) = \frac{1}{2}\Big[\left(T_W \mathrm{M}_n(\cdot,t)\right)(x) - \mathrm{d}_W(x) \mathrm{M}_n(x,t) \Big]. \tag{5.20}
$$

We can easily retrieve the equations governing the first and second order moments, as well as the one describing the behaviour of $\mathrm{Var} f$ in the limit $t \to +\infty$, which leads to the condition necessary to reach consensus. Namely:

$$
\frac{\partial \mathrm{M}_1}{\partial t}(x,t) = \frac{1}{2}\Big[\left(T_W \mathrm{M}_1(\cdot,t)\right)(x) - \mathrm{d}_W(x) \mathrm{M}_1(x,t) \Big],
$$

$$
\frac{\partial \mathrm{M}_2}{\partial t}(x,t) = \frac{1}{2}\Big[\left(T_W \mathrm{M}_2(\cdot,t)\right)(x) - \mathrm{d}_W(x) \mathrm{M}_2(x,t) \Big].
$$

The asymptotic values of the average opinion and the energy of the system are:

$$
\begin{cases}
\mathrm{M}_1^\infty = \dfrac{\left(T_W \mathrm{M}_1^\infty\right)(x)}{\mathrm{d}_W(x)} \\
\mathrm{M}_2^\infty = \dfrac{\left(T_W \mathrm{M}_2^\infty\right)(x)}{\mathrm{d}_W(x)},
\end{cases}
$$

whence:

$$
\begin{aligned}
\left(\mathrm{Var} f\right)(x,t) \xrightarrow{t\to+\infty} & \frac{\left(T_W \mathrm{M}_2^\infty\right)(x)}{\mathrm{d}_W(x)} - \frac{\Big[\left(T_W \mathrm{M}_1^\infty\right)(x)\Big]^2}{[\mathrm{d}_W(x)]^2} \\
&= \frac{1}{\mathrm{d}_W(x)}\left[\left(T_W \mathrm{M}_2^\infty\right)(x) - \frac{1}{\mathrm{d}_W(x)}\Big[\left(T_W \mathrm{M}_1^\infty\right)(x)\Big]^2 \right],
\end{aligned}
$$

Lastly, the consensus condition becomes:

$$(T_W \mathrm{M}_2^{\infty})(x) = \frac{1}{\mathrm{d}_W(x)} \Big[(T_W \mathrm{M}_1^{\infty})(x) \Big]^2, \tag{5.21}$$

which, in the spatially homogeneous case with $W \equiv 1$, reads:

$$\mathrm{m}_2(t) = (\mathrm{m}_1(t))^2 . \tag{5.22}$$

Chapter 6

Quasi-Invariant Regime and the Fokker-Planck Equation

The aim of this chapter is to explore the asymptotic behaviour of the continuous kinetic model derived in Chapter 4, specifically by analysing the system under particular scaling regimes. In principle, the system's steady state – the configuration to which it converges over long time intervals – is described by a distribution function f^∞, which satisfies the non-linear integral equation $\mathcal{Q}(f^\infty, f^\infty) = 0$. However, due to the complexity inherent in its non-linear integral structure, obtaining an analytical solution to this equation is often intractable.

To circumvent this difficulty, we seek simpler equations that approximate the full continuous model (4.10) under specific asymptotic conditions. While these scenarios are less general, they allow for analytical solutions that offer crucial insights into the system's macroscopic behaviour. These simplified configurations, known as asymptotic regimes, are typically constructed by scaling the interaction coefficients (i.e., p and q in (4.2)) by a small parameter ϵ, and subsequently taking the limit as $\epsilon \to 0^+$.

A seminal example of this approach is the grazing-collision regime introduced by Villani. Originally formulated to describe atom-atom collisions occurring at scattering angles near 180° (hence the term «grazing»), this concept was later extended by Toscani and collaborators to generic interactions, establishing the so-called QIR (Quasi-Invariant Regime). Within the QIR framework, the complex integral equation $\mathcal{Q}(f^\infty, f^\infty) = 0$ can be approximated by PDE's, such as the Fokker-Planck equation, whose properties are determined entirely by the specific scaling of the coefficients p and q.
This chapter details the derivation of the Fokker-Planck equation under the QIR scaling and analyses its implications for the networked opinion model.

6.1 Quasi-Invariant Regime and Derivation of the Fokker-Planck Equation

The main idea behind this approach is to engineer a pair of coefficients p_ϵ, q_ϵ such that the post-interaction state is negligibly affected.

Let us define the scaling parameter $0 < \epsilon \ll 1$. For symmetric interactions, the post-interaction state becomes:

$$v'_\epsilon = p_\epsilon v + q_\epsilon v_*,$$

where p_ϵ is a random variable such that:

$$\text{with:} \quad \langle p_\epsilon \rangle = 1 - \epsilon\lambda \quad \text{and} \quad \text{Var}(p_\epsilon) = \epsilon\sigma^2,$$

whereas q_ϵ is a deterministic coefficient:

$$q_\epsilon = \epsilon\lambda \in \mathbb{R}.$$

It is usual to take the following form for p_ϵ:

$$p_\epsilon := 1 - \epsilon\lambda + \sqrt{\epsilon}\sigma\eta,$$

with η being an ϵ-independent, real-valued random variable such that:

$$\langle \eta \rangle = 0, \quad \langle \eta^2 \rangle = 1 \quad \text{and} \quad \langle |\eta|^3 \rangle < +\infty.$$

Lastly, $\lambda, \sigma > 0$ are known proportionality parameters. Notice that in the QIR these coefficients are such that $p_\epsilon \to p$ and $q_\epsilon \to 0$, as $\epsilon \to 0^+$, making their definition coherent with the underlying essence of this regime.

In order to derive the Fokker-Planck equation, let us address the right-hand side of Equation (4.12). Let $v'_\epsilon = v + (p_\epsilon - 1)v + q_\epsilon v_*$. Since, in the limit $\epsilon \to 0^+$, $v'_\epsilon \approx v$, let us consider the difference $\langle \Phi(x, v') - \Phi(x, v) \rangle$ and expand it through Taylor's series centered at v with increment $v'_\epsilon - v$. Hereinafter, we will assume $\Phi \in \text{Lip}_1(\mathcal{A}) \cap \text{C}^3(\mathcal{O})$ to guarantee sufficient regularity. We obtain:

$$\begin{aligned}
\langle \Phi(x, v') - \Phi(x, v) \rangle &= \frac{\partial \Phi}{\partial v}(x, v)\Big\langle (p_\epsilon - 1)v + q_\epsilon v_* \Big\rangle + \frac{1}{2}\frac{\partial^2 \Phi}{\partial v^2}(x, v)\Big\langle (p_\epsilon - 1)v + q_\epsilon \Big\rangle^2 \\
&\quad + \frac{1}{6}\frac{\partial^3 \Phi}{\partial v^3}(x, \bar{v}_\epsilon)\Big\langle (p_\epsilon - 1)v + q_\epsilon v_* \Big\rangle^3 \\
&= \frac{\partial \Phi}{\partial v}(x, v)\Big[\underbrace{\langle p_\epsilon - 1 \rangle}_{=-\epsilon\lambda} v + \underbrace{q_\epsilon}_{=\epsilon\lambda} v_*\Big] + \frac{1}{2}\frac{\partial^2 \Phi}{\partial v^2}(x, v)\Big[\langle (p_\epsilon - 1)^2 \rangle v^2 + 2\langle (p_\epsilon - 1)q_\epsilon \rangle v v_* \\
&\quad + q_\epsilon^2 v_*^2\Big] + \frac{1}{6}\Big\langle \frac{\partial^3 \Phi}{\partial v^3}(x, \bar{v}_\epsilon)\Big[(p_\epsilon - 1)v + q_\epsilon v_*\Big]^3 \Big\rangle
\end{aligned}$$

Owing to:

$$\langle (p_\epsilon - 1)^2 \rangle = \epsilon(\sigma^2 + \epsilon\lambda^2),$$

the final form of $\langle \Phi(x, v') - \Phi(x, v) \rangle$ becomes:

$$\langle \Phi(x, v') - \Phi(x, v) \rangle = \epsilon\Big[\lambda(v_* - v)\frac{\partial \Phi}{\partial v} + \frac{1}{2}\sigma^2 v^2 \frac{\partial^2 \Phi}{\partial v^2}\Big] + \tilde{\mathcal{R}}(x, v, v_* | \bar{v}_\epsilon), \tag{6.1}$$

where:

$$\tilde{\mathcal{R}}(x,v,v_*|\bar{v}_\epsilon) := \frac{\epsilon^2\lambda^2}{2}(v-v_*)^2\frac{\partial^2\Phi}{\partial v^2}(x,v) + \frac{1}{6}\Big\langle\frac{\partial^3\Phi}{\partial v^3}(x,\bar{v}_\epsilon)\Big[(p_\epsilon-1)v+q_\epsilon v_*\Big]^3\Big\rangle. \tag{6.2}$$

In order to obtain the desired effect of the newly defined coefficients p_ϵ, q_ϵ it is necessary to scale the time as well. We define $t := \tau/\epsilon$: this allows for the creation of a new timescale (see Figure 6.1) that effectively by-passes the initial interactions that lead to the steady state in which we are interested. In so doing, we obtain a new timescale that allows the mathematical model to grasp with increasing precision the final state of the system, organically entering in the QIR.

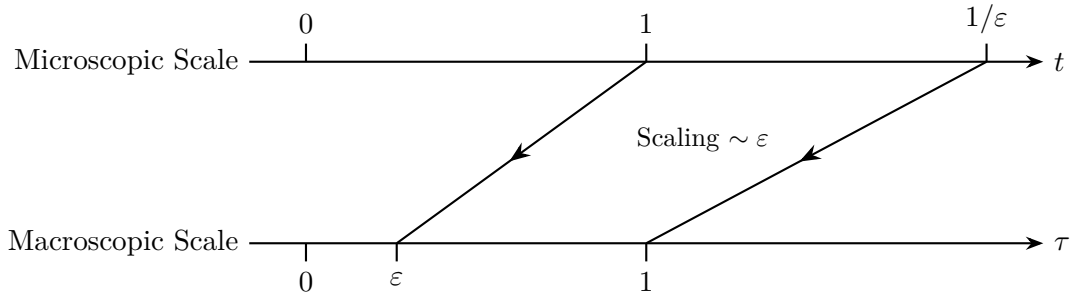

Figure 6.1. Schematic representation of the scaling limits. The microscopic time variable t is scaled by the parameter ε to obtain the macroscopic time variable τ, effectively compressing the large-scale dynamics of the kinetic model into the finite domain of the macroscopic Fokker-Planck regime

Consequently, we define:

$$f_\epsilon(x,v,\tau) := f(x,v,\tau/\epsilon), \tag{6.3}$$

leaving unaffected the space variable due to the static nature of the network structure considered. Now, consider the continuous-limit Equation (4.12). Replacing $t = \tau/\epsilon$ we get:

$$\begin{aligned}\epsilon\frac{d}{d\tau}\int_0^1\int_{\mathcal{O}}\Phi(x,v)f_\epsilon(x,v,\tau)\,dvdx = \iint_{[0,1]^2}W(x,x_*)\iint_{\mathcal{O}^2}\langle\Phi(x,v')-\Phi(x,v)\rangle \\ \times f_\epsilon(x,v,\tau)f_\epsilon(x_*,v_*,\tau)\,dvdv_*\,dxdx_*.\end{aligned} \tag{6.4}$$

Renaming $\tau \to t$ and substituting the difference (6.1) in the above Equation (6.4) we obtain:

$$\begin{aligned}\frac{d}{dt}\int_0^1\int_{\mathcal{O}}\Phi(x,v)f_\epsilon(x,v,t)\,dvdx = \frac{1}{\epsilon}\int_0^1\int_0^1 W(x,x_*)\int_{\mathcal{O}}\int_{\mathcal{O}}\epsilon\Big[\lambda(v_*-v)\frac{\partial\Phi}{\partial v}+\frac{1}{2}\sigma^2v^2\frac{\partial^2\Phi}{\partial v^2}\Big] \\ \times f_\epsilon(x,v,t)f_\epsilon(x_*,v_*,t)dvdv_*\,dxdx_* + \mathcal{R},\end{aligned}$$

where $\mathcal{R}$ is the residual part containing $\mathcal{O}(\epsilon^2)$ terms defined as:

$$\mathcal{R} := \frac{1}{\epsilon}\int_0^1\int_0^1 W(x,x_*)\int_{\mathcal{O}}\int_{\mathcal{O}}\tilde{\mathcal{R}}(x,v,v_*|\bar{v}_\epsilon)f_\epsilon(x,v,t)f_\epsilon(x_*,v_*,t)dvdv_*dxdx_*. \tag{6.5}$$

Expanding the computations and preliminarily disregarding the residual $\mathcal{R}$, the right-hand side of the above equation may be rewritten as:

$$\int_0^1\int_0^1 W(x,x_*)\Bigg[\int_{\mathcal{O}}\frac{\partial\Phi}{\partial v}f_\epsilon(x,v,t)dv\underbrace{\int_{\mathcal{O}}\lambda v_* f_\epsilon(x,v_*,t)dv_*}_{=\lambda \mathrm{M}_{1,\epsilon}(x,t)}-\underbrace{\int_{\mathcal{O}}f_\epsilon(x_*,v_*,t)dv_*}_{=1}\int_{\mathcal{O}}\frac{\partial\Phi}{\partial v}\lambda v f_\epsilon(x,v,t)dv+$$
$$+\underbrace{\int_{\mathcal{O}}f_\epsilon(x_*,v_*,t)dv_*}_{=1}\int_{\mathcal{O}}\frac{1}{2}\sigma^2v^2f_\epsilon(x,v,t)\frac{\partial^2\Phi}{\partial v^2}dv\Bigg]dxdx_*.$$

We finally arrive at the following equation:

$$\frac{d}{dt}\int_0^1\int_{\mathcal{O}}\Phi(x,v)f_\epsilon(x,v,t)\,dvdx=\int_0^1\int_0^1 W(x,x_*)\Bigg[\lambda\int_{\mathcal{O}}\frac{\partial\Phi}{\partial v}(x,v)\left(\mathrm{M}_{1,\epsilon}(x,t)-v\right)f_\epsilon(x,v,t)dv$$
$$+\frac{\sigma^2}{2}\int_{\mathcal{O}}\frac{\partial^2\Phi}{\partial v^2}(x,v)v^2f_\epsilon(x,v,t)dv\Bigg]dxdx_*, \tag{6.6}$$

which is a Fokker-Planck equation, in its weak formulation, representing the QIL (Quasi-Invariant Limit). It constitutes a much simpler equation if compared to the kinetic Equation (4.12), and – in some instances – it can be solved analytically.

As the authors in [9] report, these computations formally suggest that the equation for $f_\epsilon(t)$ approaches, as $\epsilon\to 0^+$, the following equation:

$$\frac{d}{dt}\int_0^1\int_{\mathcal{O}}\Phi(x,v)g(x,v,t)\,dvdx=\int_0^1\int_0^1 W(x,x_*)\Bigg[\lambda\int_{\mathcal{O}}\frac{\partial\Phi}{\partial v}(x,v)\left(\mathcal{M}_{1,0}(x,t)-v\right)g(x,v,t)dv$$
$$+\frac{\sigma^2}{2}\int_{\mathcal{O}}\frac{\partial^2\Phi}{\partial v^2}(x,v)v^2g(x,v,t)dv\Bigg]dxdx_*, \tag{6.7}$$

where $\mathcal{M}_{1,0}(x,t) := \lim_{\epsilon\to 0^+}\mathrm{M}_{1,\epsilon}(x,t)$. This equation is solved by a function g with the same regularity as f_ϵ, for all observables $\Phi\in \mathrm{Lip}_1(\mathcal{A})\cap \mathrm{C}^3(\mathcal{O})$. A rigorous proof of the convergence of $f_\epsilon(t)$ to $g(t)$ is sketched in [12].

6.1.1 Well-Posedness of the Quasi-Invariant Regime

In order to ensure the well-posedness of the QIR, let us start by recalling the formulation for $\tilde{\mathcal{R}}$, which is the integrand function of the residual part $\mathcal{R}$:

$$\tilde{\mathcal{R}}(x,v,v_*|\bar{v}_\epsilon) := \frac{\epsilon^2\lambda^2}{2}(v-v_*)^2\frac{\partial^2\Phi}{\partial v^2}(x,v) + \frac{1}{6}\Big\langle \frac{\partial^3\Phi}{\partial v^3}(x,\bar{v}_\epsilon)\Big[(p_\epsilon-1)v + q_\epsilon v_*\Big]^3\Big\rangle,$$

with p_ϵ, q_ϵ and η already defined.
We now aim at showing that $\mathcal{R} \overset{\epsilon\to 0^+}{\to} 0$. Taking the absolute values of both side of (6.5):

$$\begin{aligned}
|\mathcal{R}(x,v,v_*|\bar{v}_\epsilon)| &= \left|\frac{1}{\epsilon}\int_0^1\int_0^1 W(x,x_*)\int_{\mathcal{O}}\int_{\mathcal{O}} \tilde{\mathcal{R}}(x,v,v_*|\bar{v}_\epsilon) f_\epsilon(x,v,t) f_\epsilon(x_*,v_*,t) dv dv_* dx dx_*\right| \\
&= \left|\frac{\epsilon\lambda^2}{2}\int_0^1\int_0^1 W(x,x_*)\int_{\mathcal{O}}\int_{\mathcal{O}} \frac{\partial^2\Phi}{\partial v^2}(x,v)\Big[v-v_*\Big]^2 f_\epsilon(x,v,t) f_\epsilon(x_*,v_*,t) dv dv_* dx dx_*\right| \\
&\quad + \left|\frac{1}{6\epsilon}\int_0^1\int_0^1 W(x,x_*)\int_{\mathcal{O}}\int_{\mathcal{O}} \langle\frac{\partial^3\Phi}{\partial v^3}(x,\bar{v}_\epsilon)\Big[(p_\epsilon-1)v + q_\epsilon v_*\Big]^3\rangle f_\epsilon(x,v,t) f_\epsilon(x_*,v_*,t) dv dv_* dx dx_*\right|.
\end{aligned}$$

By standard estimation arguments, we get:

$$\begin{aligned}
|\mathcal{R}(x,v,v_*|\bar{v}_\epsilon)| \le{}& \frac{\epsilon\lambda^2}{2}\left\|\frac{\partial^2\Phi}{\partial v^2}\right\|_\infty \iint_{[0,1]^2}\iint_{\mathcal{O}^2} |v-v_*|^2 f_\epsilon(x,v,t) f_\epsilon(x_*,v_*,t) dv dv_* dx dx_* \\
&+ \frac{1}{6\epsilon}\left\|\frac{\partial^3\Phi}{\partial v^3}\right\|_\infty \iint_{[0,1]^2}\iint_{\mathcal{O}^2} \left|\Big\langle[(p_\epsilon-1)v + q_\epsilon v_*]^3\Big\rangle\right| f_\epsilon(x,v,t) f_\epsilon(x_*,v_*,t)\, dv dv_*\, dx dx_*.
\end{aligned}$$

After some trivial calculation that we omit, the cube of the binomial inside the angle brackets becomes:

$$\langle\Big[(p_\epsilon-1)v + q_\epsilon v_*\Big]^3\rangle = \epsilon\sqrt{\epsilon}\Big[-\epsilon^{\frac{3}{2}}\lambda^3(v-v_*)^3 - 3\epsilon^{\frac{1}{2}}\lambda\sigma^2(v-v_*)v^2 + \sigma^3\langle\eta^3\rangle v^3\Big].$$

Substituting above we obtain:

(6.8)
$$\begin{aligned}
|\mathcal{R}(x,v,v_*|\bar{v}_\epsilon)| \le{}& \frac{\epsilon\lambda^2}{2}\Big\|\frac{\partial^2\Phi}{\partial v^2}\Big\|_\infty \int_0^1\int_0^1\int_{\mathcal{O}}\int_{\mathcal{O}} |v-v_*|^2 f_\epsilon(x,v,t) f_\epsilon(x_*,v_*,t) dv dv_* dx dx_* \\
&+ \frac{1}{6}\epsilon^{\frac{1}{2}}\Big\|\frac{\partial^3\Phi}{\partial v^3}\Big\|_\infty\Big[\sigma^3\langle|\eta|^3\rangle\int_0^1\int_{\mathcal{O}}|v|^3 f_\epsilon(x,v,t) dv dx \\
&+ 3\epsilon^{\frac{1}{2}}\lambda\sigma^2\int_0^1\int_0^1\int_{\mathcal{O}}\int_{\mathcal{O}} v^2|v-v_*| f_\epsilon(x,v,t) f_\epsilon(x_*,v_*,t) dv dv_* dx dx_* \\
&+ \epsilon^{\frac{3}{2}}\lambda^3\int_0^1\int_0^1\int_{\mathcal{O}}\int_{\mathcal{O}} |v-v_*|^3 f_\epsilon(x,v,t) f_\epsilon(x_*,v_*,t) dv dv_* dx dx_*\Big].
\end{aligned}$$

Some useful bounds In the wake of the work done in [9], let us derive the following estimates.
We start by considering the first term of the right-hand side of (6.8):

$$\begin{aligned}
&\int_0^1\int_0^1\int_{\mathcal{O}}\int_{\mathcal{O}} |v-v_*|^2 f_\epsilon(x,v,t) f_\epsilon(x_*,v_*,t) dv dv_* dx dx_* \\
&\quad \le \int_0^1\int_{\mathcal{O}} v^2 f_\epsilon(x,v,t) dv dx + \int_0^1\int_{\mathcal{O}} v_*^2 f_\epsilon(x_*,v_*,t) dv_* dx_* \\
&\qquad + \int_0^1\int_0^1\int_{\mathcal{O}}\int_{\mathcal{O}} v v_* f_\epsilon(x,v,t) f_\epsilon(x_*,v_*,t) dv dv_* dx dx_* \\
&\quad \le 3\int_0^1\int_{\mathcal{O}} v^2 f_\epsilon(x,v,t) dv dx.
\end{aligned}$$

We continue by addressing the third term of (6.8), up to the multiplicative constant $3\epsilon^{\frac{1}{2}}\lambda\sigma^2$:

$$\begin{aligned}
&\int_0^1\int_0^1\int_{\mathcal{O}}\int_{\mathcal{O}} v^2 |v-v_*| f_\epsilon(x,v,t) f_\epsilon(x_*,v_*,t) dv dv_* dx dx_* \\
&\le \int_0^1\int_0^1 \left[\int_{\mathcal{O}}\int_{\mathcal{O}} v^2 |v| f_\epsilon(x,v,t) f_\epsilon(x_*,v_*,t) dv dv_* + \int_{\mathcal{O}}\int_{\mathcal{O}} v^2 |v_*| f_\epsilon(x,v,t) f_\epsilon(x_*,v_*,t) dv dv_* \right] dx dx_* \\
&= \int_0^1\int_{\mathcal{O}} |v|^3 f_\epsilon(x,v,t) dv dx + \int_0^1\int_0^1\int_{\mathcal{O}}\int_{\mathcal{O}} v^2 |v_*| f_\epsilon(x,v,t) f_\epsilon(x_*,v_*,t) dv dv_* \\
&\lesssim \int_0^1\int_{\mathcal{O}} |v|^3 f_\epsilon(x,v,t) dv dx,
\end{aligned}$$

where Hölder's inequality has been employed with indices $\mathfrak{p} = 3$ e $\mathfrak{q} = 3/2$.
In order to bound the last term of (6.8) we make use of the triangle inequality and of a combination of the results derived above to obtain:

$$\begin{aligned}
&\int_0^1\int_0^1\int_{\mathcal{O}}\int_{\mathcal{O}} |(v-v_*)^3| f_\epsilon(x,v,t) f_\epsilon(x_*,v_*,t) dv dv_* dx dx_* \\
&= \int_0^1\int_0^1\int_{\mathcal{O}}\int_{\mathcal{O}} |v^3 - 3v^2 v_* + 3v v_*^2 - v_*^3| f_\epsilon(x,v,t) f_\epsilon(x_*,v_*,t) dv dv_* dx dx_* \\
&\lesssim \int_0^1\int_{\mathcal{O}} |v|^3 f_\epsilon(x,v,t) dv dx + \int_0^1\int_0^1\int_{\mathcal{O}}\int_{\mathcal{O}} v^2 |v_*| f_\epsilon(x,v,t) f_\epsilon(x_*,v_*,t) dv dv_* dx dx_* \\
&\lesssim \int_0^1\int_{\mathcal{O}} |v|^3 f_\epsilon(x,v,t) dv dx.
\end{aligned}$$

To rigorously conclude the proof, we still need to verify that the estimates of the right-hand side of (6.8) stay bounded when $\epsilon \to 0^+$, for any fixed $t > 0$. First, let $\Phi(x,v,) = v^2$ and substitute it in Equation (6.4). We obtain:

$$\frac{d}{dt}\int_0^1\int_{\mathcal{O}} v^2 f_\epsilon(x,v,t)dvdx = \frac{1}{\epsilon}\int_0^1\int_0^1 W(x,x_*)\int_{\mathcal{O}}\int_{\mathcal{O}} \underbrace{\langle (v'_\epsilon)^2 - v^2\rangle}_{(v'_\epsilon)=p_\epsilon v+q_\epsilon v_*} f_\epsilon(x,v,t)f_\epsilon(x_*,v_*,t)dvdv_*dxdx_*$$

$$= \int_0^1\int_0^1 W(x,x_*)\left[\sigma^2\int_{\mathcal{O}} v^2 f_\epsilon(x,v,t)dv + \int_{\mathcal{O}} v^2 f_\epsilon(x,v,t)dv\,(\epsilon\lambda-1)\,2\lambda + \mathrm{M}^2_{1,\epsilon}(x)\,(1-\epsilon\lambda)\,2\lambda\right]dxdx_*$$

$$= \int_0^1\int_0^1 W(x,x_*)\left[\sigma^2\int_{\mathcal{O}} v^2 f_\epsilon(x,v,t)dv - 2\lambda\,(1-\epsilon\lambda)\left(\int_{\mathcal{O}} v^2 f_\epsilon(x,v,t)dv - \mathrm{M}^2_{1,\epsilon}(x)\right)\right]dxdx_*$$

$$\leq \int_0^1\int_0^1 W(x,x_*)\sigma^2\int_{\mathcal{O}} v^2 f_\epsilon(x,v,t)dvdxdx_* = \sigma^2\int_0^1 \mathrm{d}_W(x)\int_{\mathcal{O}} v^2 f_\epsilon(x,v,t)dvdx,$$

where we have used that $\epsilon < \frac{1}{\lambda}(1-\frac{\sigma^2}{2\lambda}) \Rightarrow 2\lambda(1-\epsilon\lambda) > 0$, by hypothesis. Exploiting the estimate $\mathrm{d}_W(x) \leq 1$:

$$\frac{d}{dt}\int_0^1\int_{\mathcal{O}} v^2 f_\epsilon(x,v,t)dvdx \leq \sigma^2\int_0^1\int_{\mathcal{O}} v^2 f_\epsilon(x,v,t)dvdx =: \sigma^2\mathrm{G}(t),$$

whence, applying Grönwall's inequality:

$$\mathrm{G}(t) \leq \mathrm{G}(0)e^{\sigma^2 t},\ \forall t\in[0,T],$$

which implies that $\mathrm{G}(t)$ stays limited, for any fixed $0 \leq t \leq T$, as $\epsilon \to 0^+$.

Let now $\Phi(x,v) = |v|^3$.

$$\frac{d}{dt}\int_0^1\int_{\mathcal{O}} |v|^3 f_\epsilon(x,v,t)dvdx = \frac{1}{\epsilon}\int_0^1\int_0^1 W(x,x_*)\int_{\mathcal{O}}\int_{\mathcal{O}}\langle |v'_\epsilon|^3 - |v|^3\rangle f_\epsilon(x,v,t)f_\epsilon(x_*,v_*,t)dvdv_*dxdx_*$$

$$\begin{aligned}= \int_0^1\int_0^1 W(x,x_*)\Bigg[&\epsilon^2\lambda^3\int_{\mathcal{O}}\int_{\mathcal{O}}\Big[|v_*|-|v|\Big]^3 f_\epsilon(t)f^*_\epsilon(t)dvdv_*\\ &+\epsilon\lambda^2\int_{\mathcal{O}}\int_{\mathcal{O}}\Big[3|v|^3 - 6v^2|v_*| + 3|v|v_*^2\Big]f_\epsilon(t)f^*_\epsilon(t)dvdv_*\\ &+\lambda\int_{\mathcal{O}}\int_{\mathcal{O}}\Big[-3|v|^3 + 3v^2|v_*|\Big]f_\epsilon(t)f^*_\epsilon(t)\\ &+\sigma^2\epsilon\lambda\int_{\mathcal{O}}\int_{\mathcal{O}}\Big[|v|^3 + 3v^2|v_*|\Big]f_\epsilon(t)f^*_\epsilon(t)dvdv_*\\ &+\Big(3\sigma^2+\epsilon^{\frac{1}{2}}\sigma^3\Big)\int_{\mathcal{O}}\int_{\mathcal{O}}|v|^3 f_\epsilon(t)f^*_\epsilon(t)dvdv_*\Bigg].\end{aligned}$$

After some calculations that we omit and using Grönwall's inequality again we obtain:

$$\frac{d}{dt}\int_0^1\int_{\mathcal{O}} |v|^3 f_\epsilon(x,v,t)dvdx \leq \mathrm{C}_{\lambda,\sigma}\int_0^1\int_{\mathcal{O}} |v|^3 f_\epsilon(x,v,t)dvdx =: \mathrm{C}_{\lambda,\sigma}\mathrm{H}(t),$$

which implies that:

$$\mathrm{H}(t) \leq \mathrm{H}(0)e^{\mathrm{C}_{\lambda,\sigma}t}, \forall t\in[0,T]$$

Finally, we have shown that:

$$\left|\mathcal{R}(x, v, v_*|\bar{v}_\epsilon)\right| \xrightarrow{\epsilon \to 0^+} 0.$$

6.2 Strong Form and Comparison with the Standard Model without Graph

In the wake of the computations located in A.2, the strong form of the Fokker-Planck equation (6.7) is:

$$\frac{\partial g}{\partial t} + \mathrm{d}_W(x)\frac{\partial}{\partial v}\Big[\lambda\left(\mathcal{M}_{1,0}(x,t) - v\right) g\Big] = \mathrm{d}_W(x)\frac{\sigma^2}{2}\frac{\partial^2}{\partial v^2}\left(v^2\, g\right), \tag{6.9}$$

Notice that d_W appears as a factor multiplying the convective and diffusive terms: this highlights the role connectivity plays during interactions. In the case a node were isolated, then we would have that $\frac{\partial g}{\partial t} = 0$, meaning that no change occurs. On the other hand, when $\mathrm{d}_W(x) > 0$ the advection and diffusion processes start to affect the distribution g, having a larger impact the closer $\mathrm{d}_W(x)$ to 1. When $\mathrm{d}_W(x) \equiv 1$, $\forall x \in [0,1]$, meaning that any couple of agents is allowed to interact without restrictions imposed by an underlying graph, we actually obtain the Fokker-Planck equation related to the standard model without an underlying graph mediating the interactions, as the authors in [9] show.

Chapter 7

Numerical Simulations

In the previous sections, we established the analytical properties of the kinetic model, characterizing the time evolution of statistical moments and providing conditions for the existence of asymptotic equilibrium states. To corroborate these theoretical findings and explore the transient dynamics that are analytically inaccessible, we now turn to a series of numerical investigations. The primary objective of this section is the following. We investigate the influence of specific network topologies – encoded by pre-determined graphons $W(x, x_*)$ – on the speed and nature of consensus formation. Furthermore, we study how a Bounded Confidence Model (BCM) leads to the formation of clusters of opinions. We employ a Direct Simulation Monte Carlo (DSMC) scheme, adapted for the graphon framework. Additionally, the simulations include the computation of the numerical error between a piecewise constant graphon W_N and a given continuous graphon W, with the assumption that W_N is obtained through a sampling process of its continuous limit. The errors are computed with respect to different norms, and are plotted using a logarithmic scale against the number of nodes that characterize W_N. Lastly, a three-dimensional comparison between W_N and W is proposed with the purpose of visually illustrating the convergence process. All the simulations are conducted using the software Matlab.

7.1 The Ochrombel Model

We consider the Ochrombel interaction model (5.19) and implement it via a DSMC method. Interactions are mediated by a piecewise constant graphon W_N sampled from the arbitrarily chosen symmetric, continuous graphon:

$$W(x, x_*) = xx_*.$$

The entries of W_N thus define the interaction probability between nodes X_i and X_j, respectively. Self-loops are not considered as we are interested in examining the opinion distributions arising from interactions among different agents.
Instead, the BCM represents a slight variation on the theme, where interactions are allowed only between individuals whose opinions differ by a bounded amount. Namely, letting p_{conf} be the confidence interval's dimension, the post-interaction state becomes:

$$v' = v'_* = v\ \chi(|v - v_*| \leq p_{\text{conf}}),$$

where $\chi(|v-v_*| \leq p_{\text{conf}}) = 1$ if $|v-v_*| \leq p_{\text{conf}}$, and it is null otherwise. This modification possibly allows for a description of those societies in which opinions may not be free to circulate and may be subjected to censorship whenever they misalign from the dominating idea by too big of a margin.

7.1.1 Results

Hereinafter, we will consider an initial opinion state randomly drawn from a uniform distribution on the interval $[-1,1]$. We start by considering a population of $N = 10^4$ individuals. Multiple conditions of interactions will be considered and their differences analysed.

Free interactions Let us first consider the case in which agents are allowed to interact freely among each other, without any restriction, i.e. p_{conf} will be chose such that $p_{\text{conf}} > \dim(\mathcal{O})$. The total number of time iterations has been chosen a-posteriori to guarantee proper convergence of the interaction model.
The final opinion distribution and the time evolution of mean opinion and standard deviation are displayed below:

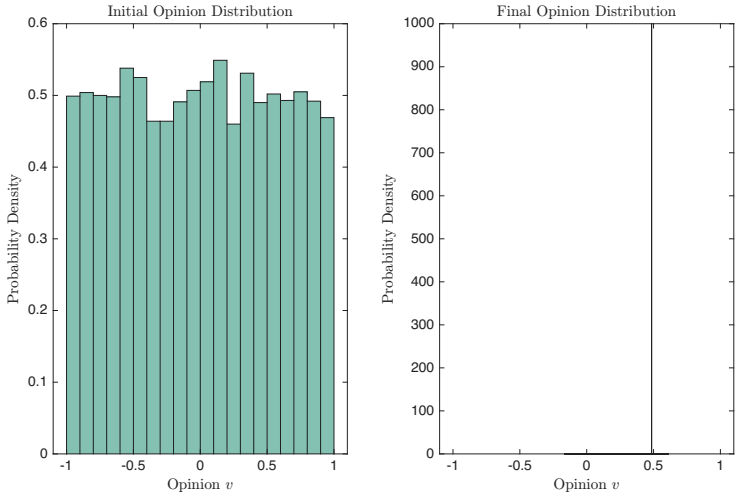

Figure 7.1. Comparison between initial opinion state (left) and final opinion state (right). Case of free interactions

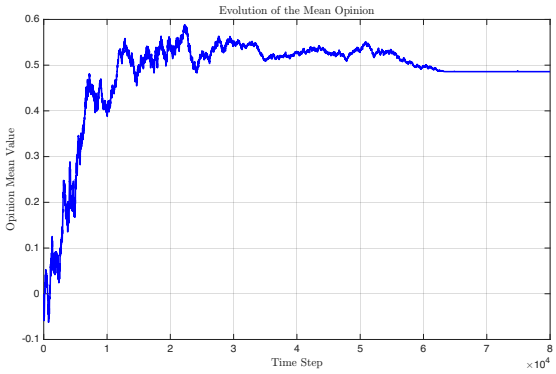

Figure 7.2. Evolution of the mean opinion state during the time interval $[0, T]$. Case of free interactions

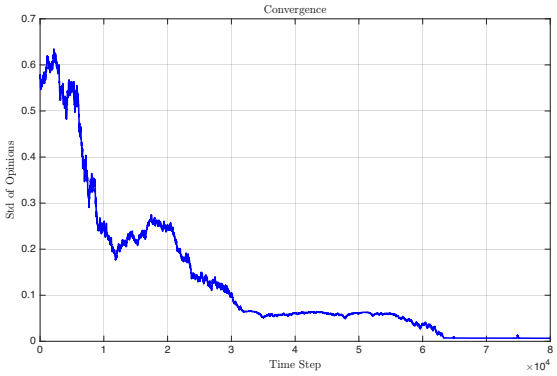

Figure 7.3. Evolution of the standard deviation of the opinion state during the time interval $[0, T]$. Case of free interactions

Figures 7.2 and 7.3 show that, in this configuration, approximately $T = 8 \cdot 10^4$ time iterations are necessary to reach consensus with final opinion state equal to $4.86 \cdot 10^{-1}$. Indeed, Figure 7.1 (right) clearly shows that the population has reached a single opinion state, namely consensus.

Bounded Confidence Interactions By progressively tweaking the BCM parameter $p_{\text{conf}} \in \{0.5, 0.75, 1\}$ we obtain the formation of clusters whose number is inversely proportional to the magnitude of the BCM parameter. Letting $p_{\text{conf}} = 0.5$ we obtain:

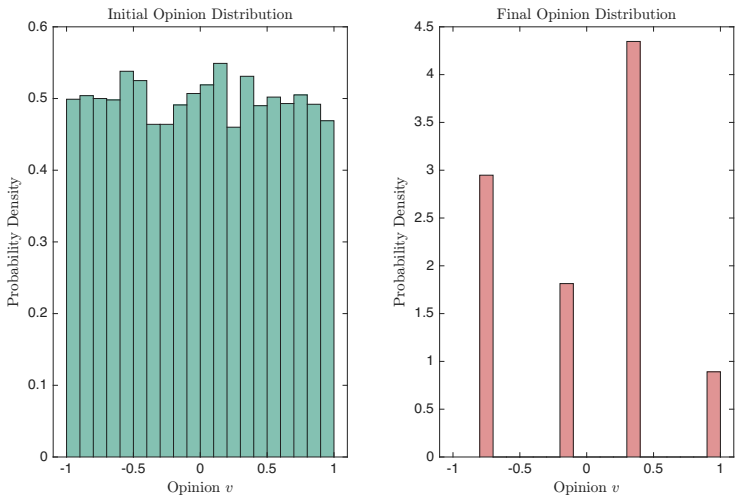

Figure 7.4. Comparison between initial opinion state (left) and final opinion state (right). Case of bounded interactions with $p_{\text{conf}} = 0.5$

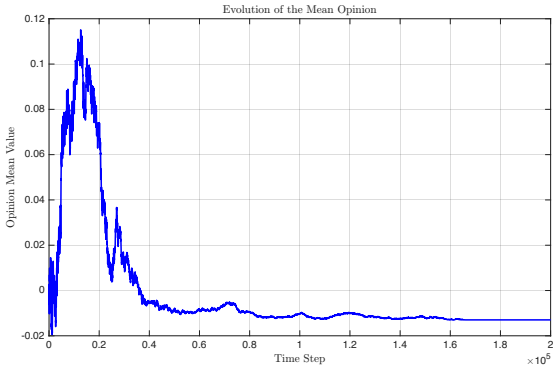

Figure 7.5. Evolution of the mean opinion state during the time interval $[0, T]$. Case of bounded interactions with $p_{\text{conf}} = 0.5$

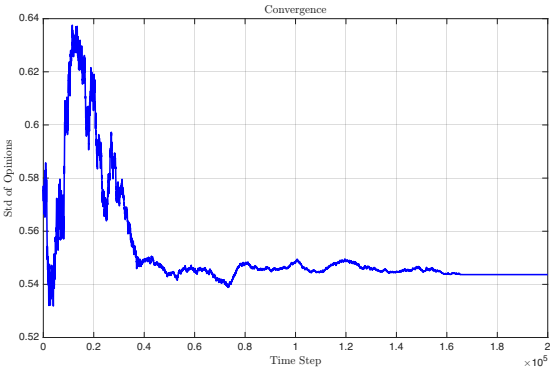

Figure 7.6. Evolution of the standard deviation of the opinion state during the time interval $[0, T]$. Case of bounded interactions with $p_{\text{conf}} = 0.5$

Figure 7.4 depicts the opinion state at the final time iteration $T = 2 \cdot 10^5$, exhibiting four peaks that represent the states towards which the system converges.
Figure 7.5 represents the mean opinion's trend. Starting at around iteration $4 \cdot 10^4$ we notice that the values begin to settle around the final value of $-1.29 \cdot 10^{-2}$, though with significant oscillations until iteration $1.4 \cdot 10^5$.
Lastly, Figure 7.6 shows the evolution of the standard deviation. We see that it does not converge to zero, not even during all the time iterations, i.e. consensus is not reached. This final configuration is the direct result of the restrictions imposed on the exchange of different opinions – agents can interact only when their position on the horizontal axis in Figure 7.4 falls under a pre-determined threshold, i.e. $p_{\text{conf}} = 0.5$. Finally, we notice a significant increase in the number of interactions needed to obtain a stable configuration.

When we take $p_{\text{conf}} = 0.75$ we observe a lower general degree of complexity regarding the convergence to a stable configuration. Indeed:

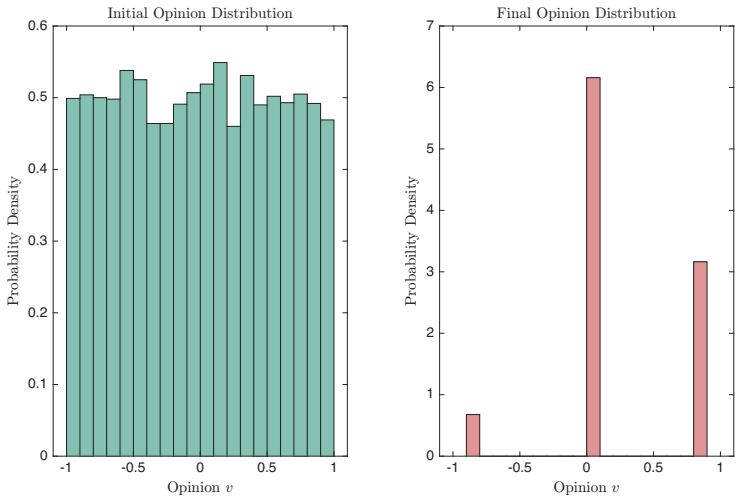

Figure 7.7. Comparison between initial opinion state (left) and final opinion state (right). Case of bounded interactions with $p_{\text{conf}} = 0.75$

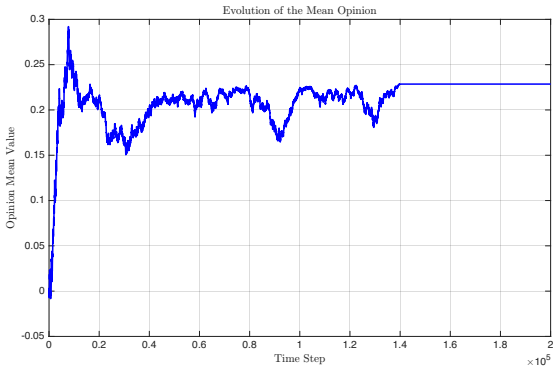

Figure 7.8. Evolution of the mean opinion state during the time interval $[0, T]$. Case of bounded interactions with $p_{\text{conf}} = 0.75$

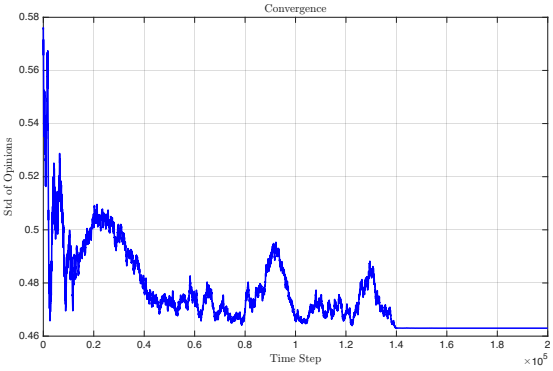

Figure 7.9. Evolution of the standard deviation of the opinion state during the time interval $[0, T]$. Case of bounded interactions with $p_{\text{conf}} = 0.75$

Figure 7.7 now shows that only three clusters have formed, represented by the three peaks. Furthermore, we notice from Figures 7.8 and 7.9 that much less time iterations were required to reach a stable layout if compared to the case with $p_{\text{conf}} = 0.5$.

Finally, letting $p_{\text{conf}} = 1$ we obtain the following results:

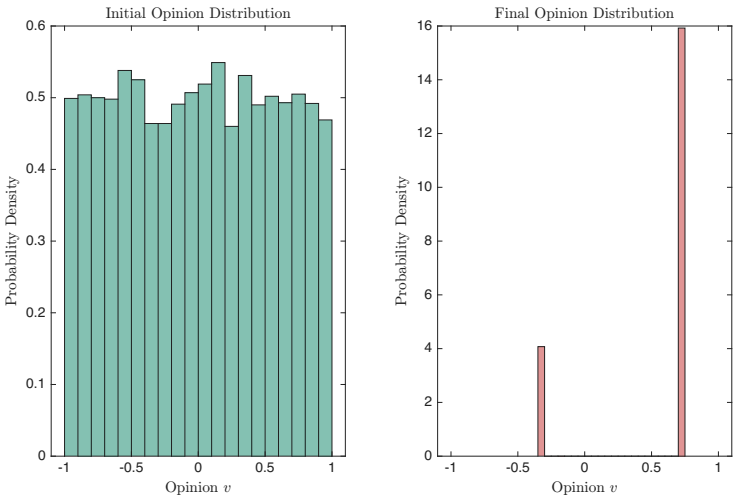

Figure 7.10. Comparison between initial opinion state (left) and final opinion state (right). Case of bounded interactions with $p_{\text{conf}} = 1$

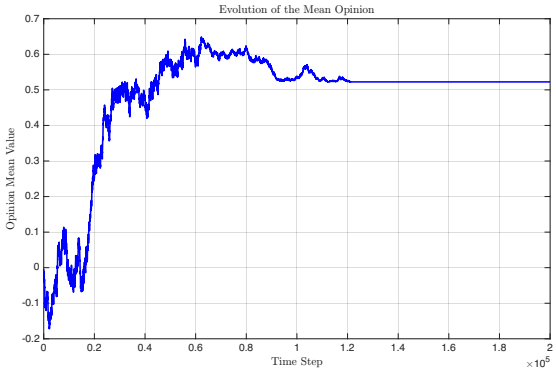

Figure 7.11. Evolution of the mean opinion state during the time interval $[0, T]$. Case of bounded interactions with $p_{\text{conf}} = 1$

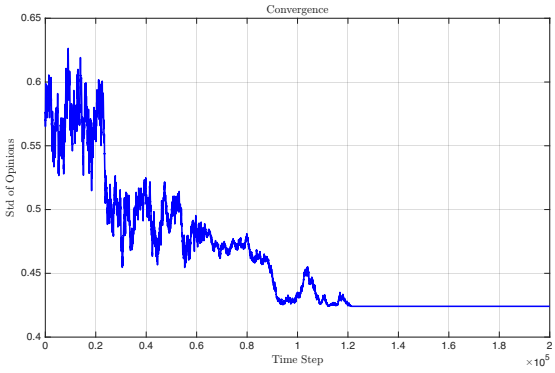

Figure 7.12. Evolution of the standard deviation of the opinion state during the time interval $[0, T]$. Case of bounded interactions with $p_{\text{conf}} = 1$

Figure 7.10 confirms the presence of the pattern theorized above – the higher the parameter p_{conf}, the lower will be the number of clusters formed through the dynamics. In addition, the lower the value of p_{conf}, the quicker a stable configuration will be achieved, as supported by the data in Figure 7.11 and Figure 7.12 where the plateau is reached at around time iteration $1.2 \cdot 10^5$ in both instances.

Remark 7.1.1 (Non-Conservativity of the Ochrombel Model)**.** *Unlike conservative models where the final consensus is determined by the initial average opinion, the Ochrombel model's dynamics are non-conservative. As seen in Figures 7.1,7.4, 7.7 and 7.10, while the initial distribution has mean value $\bar{v} = 0$ the stochastic nature of the persuasion mechanism allows the system to drift and possibly reach a consensus represented by a value*

v not necessarily equal to zero. This confirms that the first moment $\mathrm{m}_1(t)$ *is* not *an invariant of motion in this regime.*

7.2 Numerical Convergence of Graphons

In this section we validate the discrete-to-continuous transition of the network structure, a fundamental assumption that was made during the derivation phase of the continuous kinetic model. As mentioned in Chapter 3, the derivation of the mean-field limit relies on the convergence of a sequence of piecewise constant graphons $\{W_N\}_N$ to the continuous graphon W, as $N \to +\infty$.

To verify this, we used the method of manufactured solutions. We construct a target graphon W, specifically $W(x, x_*) = x\,x_*$, and generate a sequence of approximating piecewise constant graphons $\{W_N\}_N$ of increasing resolution. The error between the two representations is quantified by means of three distinct metrics: the Lebesgue L^2 Norm, the Lebesgue L^1 norm and the Cut Norm.

As far as the implementation is concerned, we chose a fine partition of $N_f = 10^3$ elements and a coarse partition of $N_c \in \{5, 10, 20, 50, 100, 200, 500, 1000\}$ nodes. After computing the difference $W_N - W$, the three errors were calculated and they are shown below:

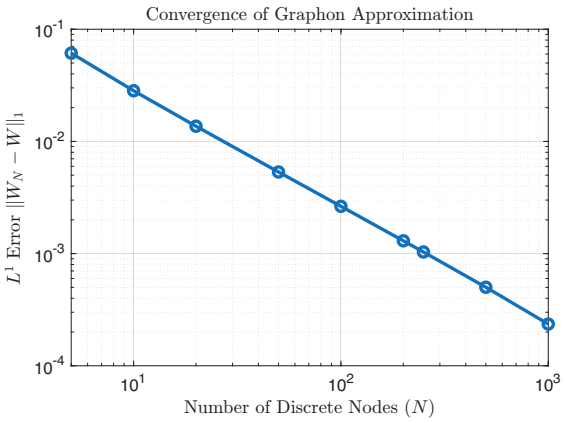

Figure 7.13. Trend of the L^1 Norm error

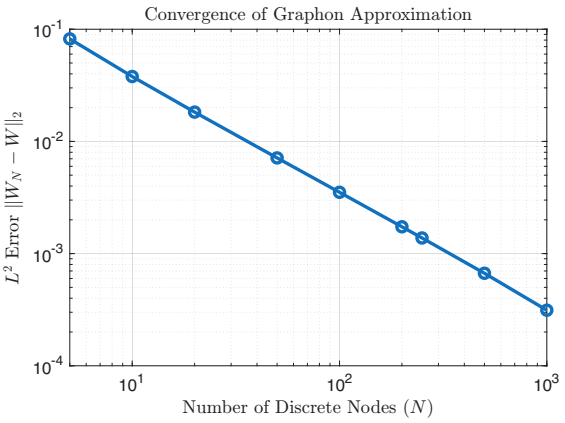

Figure 7.14. Trend of the L^2 Norm error

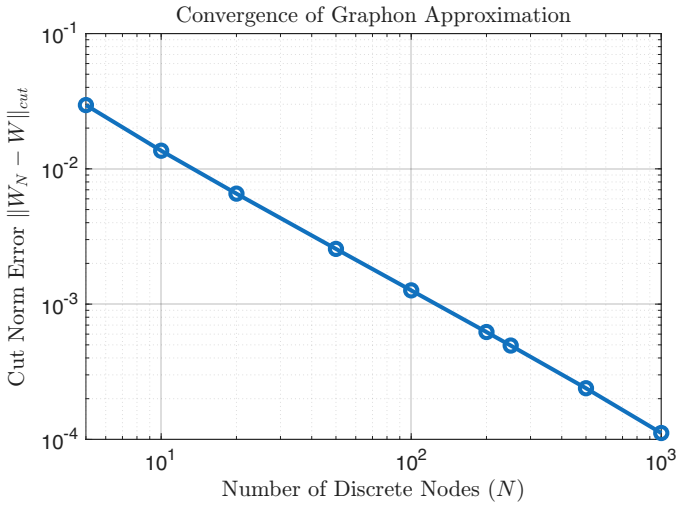

Figure 7.15. Trend of the Cut Norm error

Through Figures 7.13, 7.14 and 7.15 it is possible to notice that there exists a hierarchy among the errors, namely:

$$\|W\|_{\square} \leq \|W\|_{L^1([0,1]^2)} \leq \|W\|_{L^2([0,1]^2)},$$

thus verifying some well-known results from the general theory of graphons (see [8, Section 8.2]) and the findings of Chapter 3. Furthermore, they show, via logarithmic scale, the that the errors follow the trend $N^{-\alpha}$, with the values of α being summarized in Table 7.1.

Table 7.1. Estimated numerical convergence rates for the discrete graphon approximation

Metric	**Estimated Slope (α)**
L^2 Norm	-1.1129
L^1 Norm	-1.1056
Cut Norm	-1.1157

The results in Table 7.1 show that each norm follows a power law $N^{-\alpha}$ with $\alpha \approx -1.1$. This super-linear convergence confirms that the deterministic discretization scheme employed in our simulations is consistent, ensuring that the microscopic particle dynamics faithfully represent the continuous graphon limit described in Chapter 4.

Lastly, to better help visualizing the convergence process, we provide a comparison between the piecewise constant graphon W_N, with $N \in \{25, 100, 400\}$, and the given continuous graphon $W(x, x_*) = x\, x_*$.

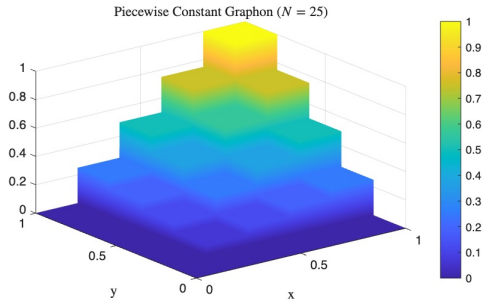

Figure 7.16. Piecewise constant graphon W_N, with $N = 25$

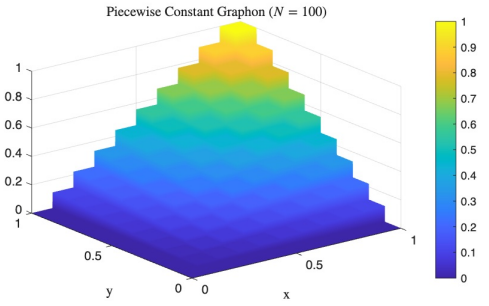

Figure 7.17. Piecewise constant graphon W_N, with $N = 100$

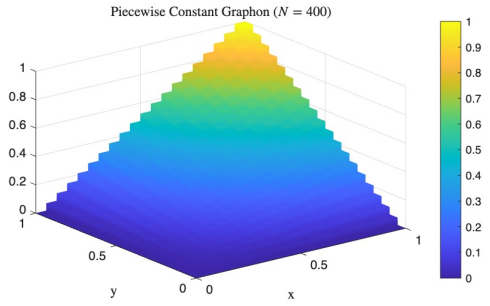

Figure 7.18. Piecewise constant graphon W_N, with $N = 400$

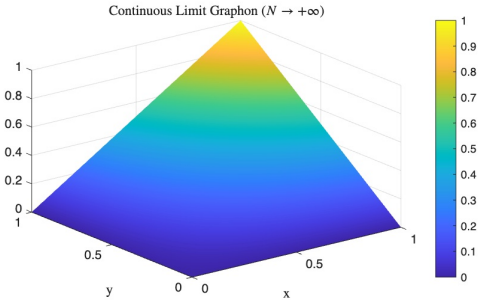

Figure 7.19. Continuous graphon $W(x, x_*) = x\, x_*$

From Figures 7.16, 7.17 and 7.18 we can see that W_N progressively better resembles its continuous limit W, depicted in Figure 7.19. These numerical results corroborate the theoretical findings in [11] about convergence of a sampled graphon to its continuous counterpart.

Chapter 8

Conclusions

This last chapter holds a summary of all the main findings of the thesis, highlighting the theoretical derivations and the numerical results presented in the previous chapters. We first review the key contributions regarding the discrete-to-continuous transition. Subsequently, we propose potential avenues for future research, emphasizing how the present framework can be extended to dynamic topologies and population control problems.

8.1 Summary of Contributions

Opinion Dynamics Modelling social dynamics presents a significant challenge due to the escalating complexity of agent connections and interactions. Describing these connections via graphons is not merely a justifiable abstraction; it provides a rigorous method to preserve the structural information of the underlying finite graph within the limit $N \to +\infty$. In this work, we began by establishing a suitable discrete framework, embedding the finite set of nodes $\mathcal{I}$ into the continuous interval [0,1] through a normalization procedure. The transition from the discrete environment to the continuous limit was achieved by linking the discrete adjacency matrix $A^{(N)}$ of the finite graph $\mathcal{G}_N$ to the continuous graphon W via the piecewise constant approximation:

$$W_N(x, x_*) = \sum_{i=1}^{N} \sum_{j=1}^{N} A_{ij}^{(N)} \chi_{I_i}(x) \chi_{I_j}(x_*).$$

Having rigorously defined the continuous setting – introducing the degree function $\mathrm{d}_W(x)$, the integral operator T_W, and the relevant modes of convergence – we proceeded to the derivation of the model.

Rigorous Derivation of the Continuous Model We introduced a piecewise-defined probability density function:

$$f_N(x, v, t) = \sum_{k=1}^{N} g_k(v, t) \chi_{I_k}(x),$$

to describe the microscopic state (x, v) at time t. The probability density function $g_k(v, t)$ describes the opinion distribution at time t of the k-th node. Utilizing the Wasserstein-$\mathcal{W}_1$ distance to quantify the convergence of f_N to its continuous limit f, we derived the discrete time-evolution equation using standard kinetic theory arguments. Notably, the inclusion of W_N in the interaction random variable $\theta \sim \text{Bernoulli}(W_N(X_i, X_j)\Delta t)$ yielded a kernel that aligns exactly with the piecewise constant graphon, offering early insights into the role of topology in the overall dynamics.

Following a heuristic formulation of the limit equation, we rigorously proved that, under reasonable assumptions regarding the convergence of the network structure and the initial distribution, the solution to the discrete equation converges to the continuous solution f in the Wasserstein sense.

Regarding the convergence of the graph sequence $(W_N)_N$ to the limit W, we examined the problem from multiple perspectives. Initially, we addressed the issue using the strongest available metric, the Lebesgue L^2 norm. Subsequently, we introduced the Cut Norm – a metric naturally more suited to this class of problems – at the expense of requiring bounds in the Lebesgue L^1 norm. Ultimately, we established a formulation relying exclusively on the Cut Norm, subject to an additional hypothesis on the convergence rate of the sequence $(W_N)_N$.

Analyses and Further Elaborations The mathematically justified continuous model was then subjected to extensive corroboration. We first verified its consistency by reducing it, via a specific choice of test function Φ, to the well-known *Repelling Dynamics* model referenced in [11]. Furthermore, we conducted a thorough analysis of the statistical moments, deriving the evolution equations for the n-th order moment $\mathrm{M}_n(x, t)$, with particular focus on the first (M_1) and second (M_2) moments. After characterizing the existence of equilibrium states M_1^∞ and M_2^∞, we investigated the consensus state, deriving the precise mathematical conditions required for its emergence. In parallel, we demonstrated that the spatially inhomogeneous model consistently reduces to the standard homogeneous case under the simplifying hypothesis $W \equiv 1$.

The Quasi-Invariant Regime In the context of Quasi-Invariant interactions, we derived the corresponding Fokker-Planck equation for the inhomogeneous model. Once again, we successfully retrieved the classical homogeneous Fokker-Planck equation under the hypothesis $W \equiv 1$, a result that corroborates the well-posedness of our derived model as a generalization of the standard framework.

Numerical Simulations Finally, we turned our attention to numerical simulation. Adopting a simplified interaction scheme, namely the Ochrombel regime, we visualized the time-evolution of the dynamics governed by Equation (4.10). We extended this analysis to include a Bounded Confidence Model, enabling the description of societies where opinion exchange is constrained by diverse confidence thresholds. In addition, we investigated the convergence error between the sampled piecewise constant graphon W_N and the continuous limit W – using a log-log analysis, we estimated the convergence rates and tabulated the results. Lastly, we provided a visual representation of the process through a

sequence of approximations showing the convergence of the piecewise constant graphons W_N to the limit W at increasing resolutions.

8.2 Limitations and Future Works

Dynamic Graphons and Adaptive Networks The present model describes interactions among agents whose connections are assumed to be static over time. In real-world scenarios, however, social ties are dynamic – they form and dissolve in response to the agents' states. A natural mathematical extension of this work is to couple the kinetic Equation (4.10) with a time-evolution equation for the graphon itself, i.e., $W = W(x, x_*, t)$. A particularly interesting phenomenon to investigate would be the decay of connectivity between agents whose mean opinions differ significantly — specifically, when $|\mathrm{M}_1(x,t) - \mathrm{M}_1(x_*,t)|$ exceeds a certain threshold. This would allow the model to capture complex social behaviours.

Data-Driven Graphon Estimation Furthermore, in Chapter 7, we assumed the limiting graphon W was known a priori. In practical applications, however, the network structure is often only observable through its finite adjacency matrix $A^{(N)}$ or through the resulting dynamics of the population. A crucial direction for future research is to devise methods to infer the underlying graphon structure from such limited data. Addressing this inverse problem would bridge the gap between kinetic theory and statistical learning, demonstrating the modern relevance of Boltzmann-type equations in the context of data science and network inference.

Optimal Control Finally, our derivation of the consensus condition highlights the topological dependence of the steady state. Future work could investigate optimal control strategies, identifying which nodes (e.g., those with high degree $\mathrm{d}_W(x)$) should be targeted to accelerate or disrupt consensus formation.

Appendix A

Proofs and Calculations

A.1 Strong form of the space-continuous Equation

Even though the weak form of Equation (4.12) is much more useful – both generally and with respect to the specific problem at hand – its strong form is more straightforward in that it gives a direct formulation for the time variation of the distribution f.
In order to transform the weak formulation into the strong one we need to manipulate Equation (4.12) and obtain a form in which we have a quantity multiplied by the test function Φ and integrated over the domain $\mathcal{A} := [0,1] \times \mathcal{O}$.
Firstly, we notice that the left-hand side of Equation (4.12) is such that:

$$\frac{d}{dt}\int_0^1 \int_{\mathcal{O}} \Phi(x,v) f(x,v,t) dv dx = \int_0^1 \int_{\mathcal{O}} \Phi(x,v) \frac{\partial f}{\partial t}(x,v,t) dv dx,$$

owing to the time independence of x e v.

As for the right-hand side:

$$\begin{aligned} &\int_0^1 \int_0^1 \int_{\mathcal{O}} \int_{\mathcal{O}} W(x,x_*)(\Phi(x,v') - \Phi(x,v)) f(x,v,t) f(x_*,v_*,t) dv dv_* dx dx_* \\ &= \underbrace{\int_0^1 \int_0^1 \int_{\mathcal{O}} \int_{\mathcal{O}} \Phi(x,v') W f f^* dv dv_* dx dx_*}_{:=\mathrm{I}^+(f,f)} - \underbrace{\int_0^1 \int_0^1 \int_{\mathcal{O}} \int_{\mathcal{O}} \Phi(x,v) W f f^* dv dv_* dx dx_*}_{:=\mathrm{I}^-(f,f)}. \end{aligned}$$

The term $\mathrm{I}^-(f,f)$ is already in the desired form:

$$\begin{aligned} \mathrm{I}^-(f,f) &= \int_0^1 \int_{\mathcal{O}} \Phi(x,v) \left[\int_0^1 \int_{\mathcal{O}} W(x,x_*) f(x,v,t) f(x_*,v_*,t) dv_* dx_* \right] dv dx \\ &= \int_0^1 \int_{\mathcal{O}} \Phi(x,v) \mathcal{Q}^-(f,f) dv dx. \end{aligned} \tag{A.1}$$

The term $\mathrm{I}^+(f,f)$, as the authors of [9] did, requires a change of variables. Letting the post-interaction variables be v and the pre-interaction variables $'v$ we get:

$$\begin{aligned}\mathrm{I}^+(f,f) &= \int_0^1\int_0^1\int_{\mathcal{O}}\int_{\mathcal{O}} \Phi(x,v')W(x,x_*)f(x,v,t)f(x_*,v_*,t)dvdv_*dxdx_* \\ &= \int_0^1\int_{\mathcal{O}} \Phi(x,v)\left[\int_0^1\int_{\mathcal{O}} \frac{1}{|J|}W(x,x_*)f(x,' v,t)f(x_*,' v_*,t)dv_*dx_*\right]dvdx \\ &= \int_0^1\int_{\mathcal{O}} \Phi(x,v)\mathcal{Q}^+(f,f)dvdx,\end{aligned}$$

where $|J|$ is the Jacobian of the transformation associated to the change of variables. To sum up:

$$\frac{\partial f}{\partial t}(x,v,t) = \mathcal{Q}^+(f,f) - \mathcal{Q}^-(f,f) \tag{A.2}$$

$$\mathcal{Q}^+(f,f) := \int_0^1\int_{\mathcal{O}} \frac{1}{|J|}W(x,x_*)f(x,' v,t)f(x_*,' v_*,t)dv_*dx_* \tag{A.3}$$

$$\mathcal{Q}^-(f,f) := \int_0^1\int_{\mathcal{O}} W(x,x_*)f(x,v,t)f(x_*,v_*,t)dv_*dx_*. \tag{A.4}$$

Notice that this derivation is coherent as long as the map Ψ is a diffeomorphism.

A.2 Strong form of the Fokker-Planck equation

Let $\Phi \in C_c^3([0,1]\times\mathcal{O})$. Formally, as previously mentioned, the scaled Boltzmann equation (6.4) satisfied by $f_\epsilon(x,v,t)$ converges, in the limit as $\epsilon \to 0^+$, to the following equation governed by the function denoted as $g(x,v,t)$. We recall that, in this context, we define $\mathcal{M}_{1,0}(x,t) := \lim_{\epsilon\to 0^+} \mathrm{M}_{1,\epsilon}(x,t)$. Proceeding via repeated integration by parts and observing that each boundary term vanishes due to the compact support of Φ. We have:

$$\begin{aligned}\frac{d}{dt}\int_0^1\int_{\mathcal{O}} \Phi(x,v)g(x,v,t)\,dvdx = \iint_{[0,1]^2} W(x,x_*)\Bigg[\lambda\int_{\mathcal{O}} \frac{\partial\Phi}{\partial v}(x,v)\left(\mathcal{M}_{1,0}(x,t)-v\right)g(x,v,t)dv \\ + \frac{\sigma^2}{2}\int_{\mathcal{O}} \frac{\partial^2\Phi}{\partial v^2}(x,v)v^2 g(x,v,t)dv\Bigg]dxdx_*\end{aligned}$$

Developing the computations for the right-hand side we obtain:

$$\begin{aligned}\iint_{[0,1]^2} W(x,x_*)\Bigg[\lambda\left(\mathcal{M}_{1,0}(x,t)-v\right)g(x,v,t)\underbrace{\Phi(x,v)}_{=0}\Big|_{\partial\mathcal{O}} - \int_{\mathcal{O}}\Phi(x,v)\frac{\partial}{\partial v}\Big[\lambda\left(\mathcal{M}_{1,0}(x,t)-v\right)g(x,v,t)\Big]dv \\ + \frac{\sigma^2}{2}v^2 g(x,v,t)\underbrace{\frac{\partial\Phi}{\partial v}}_{=0}\Big|_{\partial\mathcal{O}} - \int_{\mathcal{O}}\frac{\partial\Phi}{\partial v}\frac{\sigma^2}{2}\frac{\partial}{\partial v}\left(v^2\,g(x,v,t)\right)dv\Bigg]dxdx_*\end{aligned}$$

$$= - \iint_{[0,1]^2} W(x,x_*) \Bigg[\int_{\mathcal{O}} \Phi(x,v) \frac{\partial}{\partial v} \Big[\lambda \left(\mathcal{M}_{1,0}(x,t) - v \right) g(x,v,t) \Big] - \frac{\sigma^2}{2} \left(2v\, g(x,v,t) + v^2 \frac{\partial g}{\partial v} \right) \underbrace{\Phi(x,v)}_{=0} \Big|_{\partial \mathcal{O}} + \int_{\mathcal{O}} \Phi(x,v) \frac{\sigma^2}{2} \frac{\partial^2}{\partial v^2} \left(v^2\, g(x,v,t) \right) dv \Bigg] dx dx_*.$$

We notice that the only term depending on x_* is the graphon. Thus, we are able to integrate it and introduce the degree d_W of node x into the formulation:

$$\int_0^1 \int_{\mathcal{O}} \Phi(x,v) \frac{\partial g}{\partial t}\, dv dx = - \int_0^1 \int_{\mathcal{O}} \Phi(x,v) \Big[\mathrm{d}_W(x) \frac{\partial}{\partial v} \left(\lambda \left(\mathcal{M}_{1,0}(x,t) - v \right) g(x,v,t) \right) \Big] dv dx + \int_0^1 \int_{\mathcal{O}} \Phi(x,v) \Big[\mathrm{d}_W(x) \frac{\sigma^2}{2} \frac{\partial^2}{\partial v^2} \left(v^2\, g(x,v,t) \right) \Big] dv dx,$$

for all $\Phi \in C_c^3([0,1] \times \mathcal{O})$.
Switching to the strong form and rearranging the terms:

$$\frac{\partial g}{\partial t} + \mathrm{d}_W(x) \frac{\partial}{\partial v} \Big[\lambda \left(\mathcal{M}_{1,0}(x,t) - v \right) g \Big] = \mathrm{d}_W(x) \frac{\sigma^2}{2} \frac{\partial^2}{\partial v^2} \left(v^2\, g \right), \tag{A.5}$$

which is the unsteady, reaction-convection-diffusion Fokker-Planck equation.
As a side note, we can observe that when each agent is free to interact with any other agent (i.e., $\mathrm{d}_W(x) = 1$, $\forall x \in [0,1]$) we retrieve the Fokker-Planck equation obtained from the classic Boltzmann interaction model in which the notion of graph (or graphon) does not feature:

$$\frac{\partial g}{\partial t} + \frac{\partial}{\partial v} \Big[\lambda \left(\mathcal{M}_{1,0}(x,t) - v \right) g \Big] = \frac{\sigma^2}{2} \frac{\partial^2}{\partial v^2} \left(v^2\, g \right). \tag{A.6}$$

Bibliography

[1] Sebastian Allmeier and Nicolas Gast. Accuracy of the graphon mean field approximation for interacting particle systems, 2024.

[2] M. Bisi, G. Spiga, and G. Toscani. Kinetic models of conservative economies with wealth redistribution. *Communications in Mathematical Sciences*, 7(4):901–916, 2009.

[3] G. Dimarco, B. Perthame, G. Toscani, and M. Zanella. Kinetic models for epidemic dynamics with social heterogeneity. –, 2021.

[4] Bertram During, Jonathan Franceschi, Marie-Therese Wolfram, and Mattia Zanella. Breaking consensus in kinetic opinion formation models on graphons. *Journal of Nonlinear Science*, 2024.

[5] L. Hodgkinson. Graphons and convergence. –, –.

[6] Svante Janson. Graphons, cut norm and distance, couplings and rearrangements. *2000 Mathematics Subject Classification. 05C99, 28A20.*, 2011.

[7] J. L. Krivine. Constantes de grothendieck et fonctions de type positif sur les sphères. *Advances in Mathematics, Vol. 31, Issue 1, pp. 16-30*, January 1979.

[8] László Lovász. *Large Networks and Graph Limits*, volume 60 of *Colloquium Publications*. American Mathematical Society, Providence, Rhode Island, 2012.

[9] N. Loy and A. Tosin. Essentials of the kinetic theory of multi-agent systems. -, 2025.

[10] Marco Nurisso, Matteo Raviola, and Andrea Tosin. Network-based kinetic models: Emergence of a statistical description of the graph topology. *European Journal of Applied Mathematics*, 2024.

[11] Raoul Prisant, Federica Garin, and Paolo Frasca. Opinion dynamics on signed graphs and graphons. –, 2025.

[12] M. Torregrossa and G. Toscani. On a fokker–planck equation for wealth distribution. *Kinetic and Related Models*, 11(2):337–355, 2018.

[13] G. Toscani, P. Sen, and S. Biswas. Kinetic exchange models of societies and economies. *The Royal Society Publishing*, 2022.